

FORECASTING CLIMATE AND WATER RESOURCES IN THE CONTEXT OF
NATURAL VARIABILITY AND CLIMATE CHANGE

by

Matthew Switanek

A Dissertation Submitted to the Faculty of the
DEPARTMENT OF HYDROLOGY AND WATER RESOURCES

And the

DEPARTMENT OF ATMOSPHERIC SCIENCES

In Partial Fulfillment of the Requirements

For the Degree of

DOCTOR OF PHILOSOPHY

WITH A MAJOR IN HYDROMETEOROLOGY

In the Graduate College

THE UNIVERSITY OF ARIZONA

2013

THE UNIVERSITY OF ARIZONA
GRADUATE COLLEGE

As members of the Dissertation Committee, we certify that we have read the dissertation prepared by Matthew Switanek, titled Forecasting Climate and Water Resources in the Context of Natural Variability and Climate Change and recommend that it be accepted as fulfilling the dissertation requirement for the Degree of Doctor of Philosophy.

_____ Date: 4/25/2013
Peter Troch

_____ Date: 4/25/2013
Christopher Castro

_____ Date: 4/25/2013
Francina Dominguez

_____ Date: 4/25/2013
Hoshin Gupta

Final approval and acceptance of this dissertation is contingent upon the candidate's submission of the final copies of the dissertation to the Graduate College.

I hereby certify that I have read this dissertation prepared under my direction and recommend that it be accepted as fulfilling the dissertation requirement.

_____ Date: 4/25/2013
Dissertation Director: Peter Troch

STATEMENT BY AUTHOR

This dissertation has been submitted in partial fulfillment of the requirements for an advanced degree at the University of Arizona and is deposited in the University Library to be made available to borrowers under rules of the Library.

Brief quotations from this dissertation are allowable without special permission, provided that an accurate acknowledgment of the source is made. Requests for permission for extended quotation from or reproduction of this manuscript in whole or in part may be granted by the head of the major department or the Dean of the Graduate College when in his or her judgment the proposed use of the material is in the interests of scholarship. In all other instances, however, permission must be obtained by the author.

SIGNED: Matthew Switanek

ACKNOWLEDGMENTS

I thank my graduate adviser, Peter Troch, for his unwavering support and patience. He has confidence in his students abilities, which is liberating. I also appreciate the efforts of my graduate committee members, Christopher Castro, Francina Dominguez, and Hoshin Gupta.

Others along the way, that I am indebted to, are Ingo Heidbuechel, Maite Guardiola-Claramonte, Eleonora Demaria, Matej Durcik, Rachel Lambethbeagles, Patrick Broxton, Will Veatch, Caitlan Zlatos, and many other who have helped shape me professionally and personally.

DEDICATION

I would like to dedicate my efforts over the course of this program to my loving parents, Andy and Judi. They have been more supportive and understanding than I believed possible. I owe my efforts to them, and I trust that any accomplishments that I have in life are reflective of this fact. I would like to thank my brother, Nick, who has always challenged me. He has spent many hours helping me think through problems, while always providing support and love. Lastly, I thank my most beautiful betrothed, Heide Bruckner. She has made the last year of this effort enjoyable, and has helped push me with her unremitting love.

TABLE OF CONTENTS

LIST OF FIGURES.....8

ABSTRACT.....9

CHAPTER 1. INTRODUCTION.....11

CHAPTER 2. PRESENT STUDY.....15

**2.1 Improvements in Seasonal Forecasts of Precipitation Across the
 United States.....15**

 2.1.1 Methods and Results.....15

 2.1.2 A Brief History of the El Niño Southern Oscillation.....22

2.2 Decadal Forecasts of Colorado River Basin Streamflow.....35

 2.2.1 Methods and Results.....35

**2.3 Expected Affects to the Water Resources of the Southwestern
 United States Due to a Changing Climate.....40**

 2.3.1 Methods and Results.....40

2.4 Conclusions and Continuation of Research.....48

REFERENCES.....52

**APPENDIX A: AN OBJECTIVE AND CONCISE APPROACH FOR IMPROVING
SEASONAL FORECASTS OF PRECPITATION ACROSS THE UNITED
STATES.....55**

TABLE OF CONTENTS - Continued

APPENDIX B: DECADEAL PREDICTION OF COLORADO RIVER

STREAMFLOW ANOMALIES USING OCEAN-ATMOSPHERE

TELECONNECTIONS.....79

APPENDIX C: DYNAMICALLY DOWNSCALED AND BIAS-CORRECTED

CLIMATE PROJECTIONS EXHIBIT A DRIER FUTURE FOR

SOUTHWEST RIVER BASINS.....99

LIST OF FIGURES

Figure 1.....	19
Figure 2.....	20
Figure 3.....	21
Figure 4.....	26
Figure 5.....	27
Figure 6.....	28
Figure 7.....	33
Figure 8.....	37
Figure 9.....	38
Figure 10.....	39
Figure 11.....	45
Figure 12.....	46
Figure 13.....	47

ABSTRACT

The water resources of the Southwestern United States are under significant stress. The historical record of the Colorado River indicates that the commitment allocations (7.5 million acre-feet to both the Upper and Lower Colorado basin states, and 1.5 maf for Mexico) have overestimated the average available streamflow. Compounding the supply problem, the Bureau of Reclamation has projected an average decrease of 9% in the Colorado River streamflow between the years 2011-2060. Improving forecasts of climate and streamflow, at nearly all time scales, is imperative to most effectively manage these strained water resources.

Given the challenges confronting the Southwest, three research studies are presented that could be used to assist water managers. The first study targets the lack of skill seen in seasonal forecasts of precipitation across the US issued by the Climate Prediction Center (CPC). An objective and concise methodology is shown to improve overall seasonal forecast skill as an alternative to forecasts made by the CPC. This methodology uses a combined linear and nearest neighbor model to make forecasts, with the NINO3.4 index as the only predictor. The second study shows skillful forecasts of decadal Colorado streamflow using the Atlantic Multidecadal Oscillation (AMO) and Pacific Decadal Oscillation (PDO) indices as predictors. However, even though the instrumental record showed statistically significant skillful forecasts, the reconstructed records of AMO, PDO and streamflow appear to challenge these results. Lastly, the third study investigates the effects of climate change in the 21st century on the Salt, Verde and

Rio Grande river basins. Two dynamically downscaled General Circulation Models (GCMs) are first bias-corrected. Then, the output of these models is used as the climatic forcings for the Variable Infiltration Capacity (VIC) hydrologic model. Results suggest that future streamflows are projected to decrease by 22% and 37%, for the respective GCMs, averaged across the basins.

1. INTRODUCTION

Climate plays an integral role in the livelihood of the planet on which we live. Over the course of thousands of years, societies that had once flourished have subsequently, and sometimes suddenly, died out due to lack of water resource availability (Waters and Ravesloot, 2001). Water truly is a substance that is required by all life as we know it. More specifically, humans need an immense amount of fresh water. We use it for drinking, growing our food, for recreation, or to power our homes and our economic industrial framework. As a result, people have become increasingly more proactive in trying to move, control and store water for these needs. This is happening across the world, but a prime example of where the stakes are particularly high is the Southwestern United States.

The Southwestern United States is fairly unique insofar that much of it is comprised of a temperate climate which is conducive to year-round agriculture. However, these same swaths of land within the region are not necessarily adjacent (<100km) to abundant supplies of surface water. In short, an incredible amount of modern day agriculture is taking place in a region that has not natively and historically supported that amount of biological richness. In our effort to create this system of food supply that is so vital to our country, massive engineering works have been put up to sustain this dynamic. This is in addition to the dams being built to provide an economic stimulus during the Great Depression and their ability to control floods. By the year 1944, the amount of

water allocated between seven states in the Southwest, in addition to Mexico, was 16.5 maf ($\sim 2 \times 10^{10} \text{ m}^3$). The Hoover and Glen Canyon dams partition most of the water along the Colorado River. Since the Colorado River Compact in 1922 and the Mexican Water Treaty of 1944, measured streamflow has suggested that the river may be over-allocated. The Colorado River is currently the most heavily regulated and litigated river in the world. Given this strain placed on the Colorado water supply, and provided its importance to a variety of societal and economic sectors, it is imperative that we understand the seasonal, annual, inter-annual and decadal natural variability of the system (Barnett et al., 2005; Christensen et al., 2004; Milly, 2010). On top of that, a future plan that accounts for the anticipated impacts that climate change will have on the water resources of this region is undoubtedly essential to a Southwestern United States that is under duress (Rajagopalan et al., 2009; McCabe and Wolock, 2007).

As physical scientists, we often have an aversion to political and managerial policy. This potentially stems from a discomfort that we might have with subjective, amorphous matters. Unfortunately, political policy invariably trickles down to public policy and into the very communities that we live. Our role is not, and should not be, to govern what is best for the people and the environment that we care about. However, we can consider it an obligation to provide these lawmakers and resource managers with the absolute best information available. Thus, we should provide an adequate outline of what is probable, what is feasible, and what is irresponsible.

In this document, we present three research studies that attempt to shed some light

on this task, which is providing lawmakers and resource managers with information that they can use to make decisions that reflect societies' best interests.

The first study deals with seasonal climate forecasting. This is important in near-term decisions that must be made concerning water resources. Currently, weather forecasts typically are not very skillful beyond 5 to 7 days. This is due to the fact that some terms, in governing atmospheric equations, are neglected so that the system of equations may be solved. However, the contributions of these smaller terms can become large over time, and thus the skill drops off as the influence of these terms becomes more prevalent. As a result, there is an inherent limit on weather predictability. Climate is the aggregate weather over timescales of weeks, months and years. So, even though the skill in predicting actual weather events drops off after 5 days, there can still be skill in forecasting whether or not the climate (which is the time averaged weather) will be wetter, drier, warmer or cooler than average. The Climate Prediction Center of the United States is the entity that makes official forecasts of precipitation and temperature for a variety of lead times (between the next 3 month season and the 3 month season 1 year out). They have more skill in seasonal temperature forecasts (O'Lenic et al., 2008). Given the lack of skill in precipitation forecasts, and the control that precipitation has on available water resources, this study has focused on improving precipitation forecasts.

The second study moves on to make forecasts of decadal streamflow in the Colorado River. This information, for a basin like the Colorado River, is invaluable to understand whether or not shifts in allocation are required. For example, should some

amount of agriculture be fallow, or should it move somewhere else entirely. The Bureau of Reclamation is the entity responsible for the Colorado River basin. They have many contingency plans provided certain scenarios, but currently they are not implementing any skillful decadal forecasts of streamflow. The second study focuses on providing a method that makes skillful forecasts of decadal Colorado streamflow.

The third study confronts the challenging issue that climate change poses to the water resources of the Southwest. Past studies have indicated, in the Southwest, that the amount of temperature increases projected by General Circulation Models (GCMs) will more than offset any potential increases in precipitation, thus leading to less water resources. These studies used statistically downscaled GCMs. Dynamically downscaling GCMs can yield a different result, and one that captures the mechanics of the system. This last study focuses on what changes we might expect to water availability in the Southwest, due to climate change, when dynamically downscaled climate data is used.

2. PRESENT STUDY

2.1 Improvements in Seasonal Forecasts of Precipitation Across the United States

This section summarizes the methods, results and conclusions of the paper titled “An Objective and Concise Approach for Improving Seasonal Forecasts of Precipitation Across the United States.” The full document is found in Appendix A.

The Climate Prediction Center (CPC) has been making seasonal climate forecasts, at multiple lead times. They have been archiving these forecasts since late 1994. Forecasts of the CPC rely on some combination of a variety of methods. They use both statistical methods in addition to an ensemble average of a perturbed dynamical atmospheric model. Combining the different forecasts has not always been objective, and is heavily influenced by whether or not an El Niño or La Niña is present. Since precipitation forecast skill does go up during a strong El Niño or La Niña, can a completely objective and simplified methodology, that takes advantage of that fact, match or exceed the seasonal forecast skill of the CPC?

2.1.1 Methods and Results

Our study set out to observe if the level of skill historically seen by the CPC can be exceeded by using a single ENSO index in an objective and concise methodology. We used the NINO3.4 index, which is the average SST over the region 120°W-170°W and 5°S-5°N. Both a linear model and a nearest neighbors model were used in combination to provide our retrospective forecasts. The models are both being forced with only the

NINO3.4 index. As a case study, we focus on improving the forecasts of the next season of precipitation throughout the year.

A linear model uses the most recently fully completed month's NINO3.4 SSTs to make forecasts of the next season's precipitation. The model is trained on all of the available prior data. For example, the linear model is fit to the data of November (years 1901-1990) NINO3.4 SSTs and a specified climate division's precipitation for the following January-March (years 1902-1991). Then the November, 1991 NINO3.4 SST is used to forecast January-March, 1992 precipitation. Similarly to the linear model, the nearest neighbors model uses the same data to fit the model. Nearest neighbors essentially finds analogs of past events. It searches in parameter space to find the closest events of the past to the current event being used to forecast. In our model, we only have one predictor, so it will seek out the closest NINO3.4 SST values in the past with respect to the current value. Eight different models were fit, with each using the closest one nearest neighbor on through the closest eight nearest neighbors.

Forecasts are made only with models that have historically shown positive skill.

The skill measure that we used is defined as

$$\text{Skill} = r * (1 - (1 - CV)^2) \quad (1)$$

where r is the correlation coefficient between the forecasted and observed values (using the 50th percentiles of probabilistic forecasts), and CV is the ratio of the coefficient of variations of the forecasted to the observed values. Both of the models establish past skill using all of the preceding years of forecasts beginning in the year 1971. For example, if

the linear model forecasting January-March precipitation in a specified climate division had a skill measure of .2 (which is positive skill) for the years 1971-2000, then the model would be part of the overall precipitation forecast. The past skillful nearest neighbors models were averaged into a single precipitation forecast. The nearest neighbors forecast was then equally weighted with the linear model forecast to create a final forecast.

Figure 1 shows the skills for the CPC by climate division and season. Colors that are red have no skill or negative skill, while the other colors have some amount of skill with the blues being the most skillful. Figure 2 presents the skills we obtained through our methodology. Figure 2 shows, on average, more regions with increased skill over Figure 1. Figure 3 shows the spatially averaged skills for each season. Our proposed methodology performs better, as a spatial average, than the CPC for every season but ASO.

As can be seen in Figure 3, the strength of the methodology lies in two areas. First, using an extended time series (1901-2012) of NINO3.4 and precipitation gives better average skill through the year than using the last 30 years or the climatology. Second, the linear model and the nearest neighbors model both have their strengths, and when they are combined they are more skillful than either alone.

The most likely next step to further improve forecasts is to further refine which seasons and regions have more skillful forecasts when using either the most recent 1 month or 3 month average NINO3.4 as a predictor. We found that the winter season is predominantly governed by the prior 1 month's NINO3.4, while the summer season is

governed by the prior 3 month's. For the purposes of the study, and in an effort to present a simplified methodology, we use just the most recent 1 month average. However, this requires further investigation.

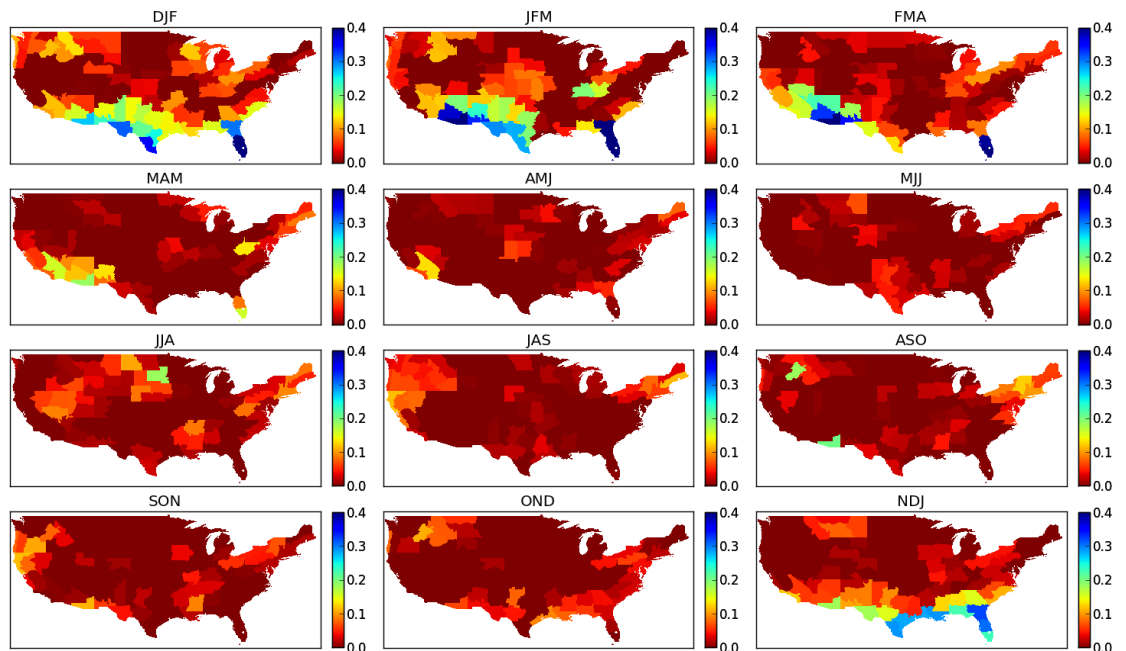


Figure 1: The CPC's next season precipitation forecast skills. Cooler colors represent higher skill, while everything that is not completely red represents some amount of skill. The regions of saturated red show that, up to date, there is no discernible forecast skill in these regions for these seasons.

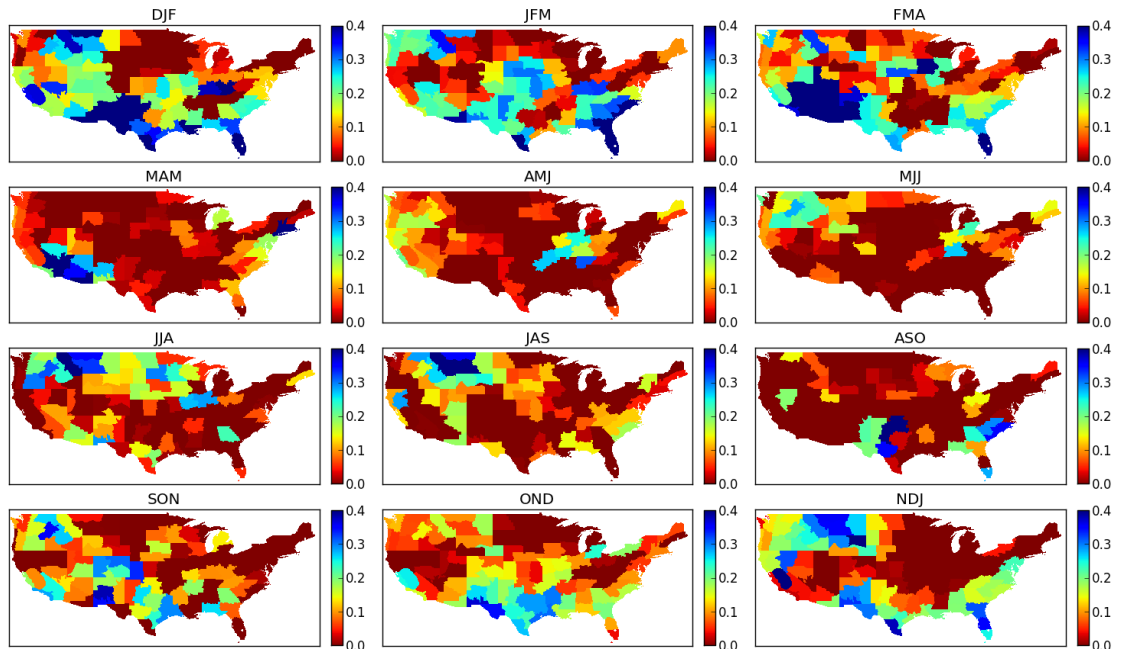


Figure 2: The spatial distribution of forecast skill by season. Here, the combined forecasts of the linear and nearest neighbor models is implemented using the most recent completed month of NINO3.4.

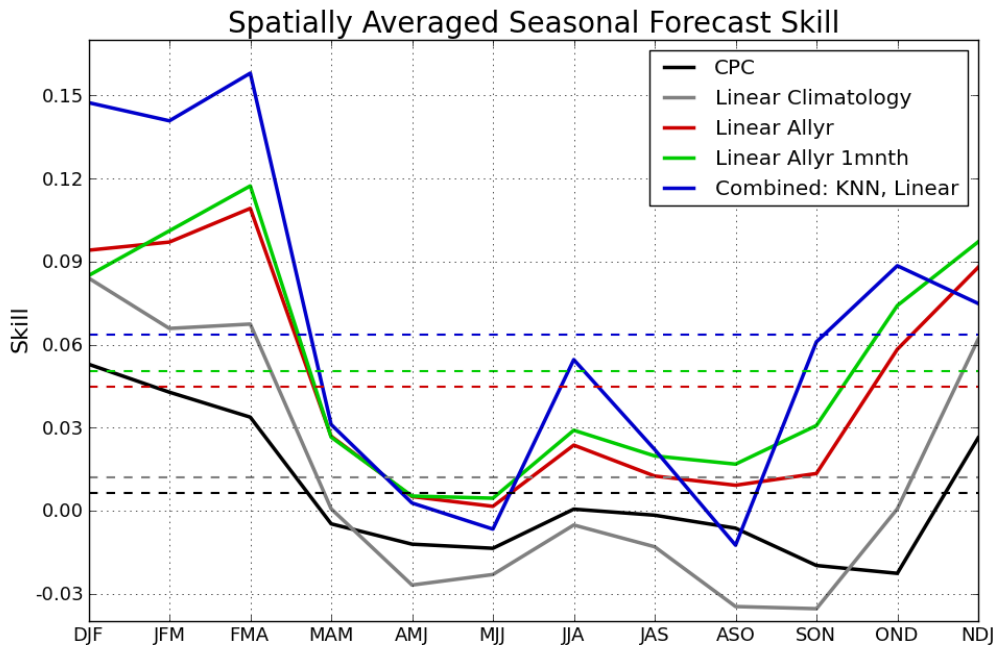


Figure 3: The CPC's average skills, by season are shown in black, while the climatological linear model that uses NINO3.4 as a predictor is the gray line. The red and green lines are the linear models using all prior values of 3 and 1 month averaged NINO3.4 and precipitation, respectively. The blue line is the resulting forecasts that incorporated both the linear model and the nearest neighbor model using all prior 1 month mean NINO3.4 SSTs .

2.1.2 A Brief History of the El Niño Southern Oscillation

In our first study, we are using the ENSO phenomenon statistically. However, it can be helpful to have an understanding of the dynamics of ENSO when interpreting the forecasts of that study. The term El Niño was originally used by fishermen along the coasts of Ecuador and Peru in reference to warmer coastal water in the Pacific. El Niño is translated as “the Christ Child” and refers to the fact that the event typically appears around Christmas time and last for several months. The fishermen noticed that in addition to there being less fish in the less nutrient rich warm water, El Niño events could also bring heavy rains.

Sir Gilbert Walker was a British scientist that first noticed, in the 1920s, a connection between barometer readings at stations on the eastern and western sides of the tropical Pacific (between Tahiti and Darwin, Australia). When pressure rises in the west, it usually falls in the east, and vice versa. The term Southern Oscillation was coined by Walker to describe this phenomenon. Later in the 1960s, Jacob Bjerknes recognized a connection between warm, tropical SSTs and weak easterlies (Bjerknes, 1969). His work led to the understanding that the warm waters of El Niño and the pressure variations of the Southern Oscillation are part of the same phenomenon, which often today is referred to as ENSO (El Niño Southern Oscillation). Figure 4 shows the relationship between the SSTs in the equatorial Pacific region NINO3.4 and the Southern Oscillation.

Since these discoveries, there has been many studies that have linked interannual climate variability to ENSO (Horel and Wallace, 1981; Livezey and Mo, 1987;

Ropelewski and Halpert, 1986). The understanding of how an ENSO event plays out physically, once it has started, has substantially improved seasonal climate forecasts, especially in the winter.

It is still unclear what creates the onset of an El Niño event. Some believe that the Pacific ocean-atmosphere has a natural frequency, or oscillation, which is perturbed by chaotic processes to be irregular. Others believe the system to be more stable and an event is triggered by some type of outside forcing. Importantly, both theories require a “build up” of the western Pacific for an El Niño, of relevant magnitude, to take place. The “build up” is the warming of the western Pacific. If there is not a large, thick warm pool of water in the western Pacific, there will not be sufficiently enough energy and mass released to the atmosphere to fuel an El Niño event (<http://faculty.washington.edu/kessler/occasionally-asked-questions.html#q12>). However, if there is a proper “build up,” then there is a feedback response once it has begun. Whether there is a weakening of the easterlies or a warming of the central to eastern equatorial Pacific that initiates the event, they both can lead to similar results. As warmer surface water moves east in the equatorial Pacific, the air mass above these waters becomes less dense and the sea level pressure decreases, and vice versa as the waters cool in the western equatorial Pacific. As a result, there is a shift in where the pressure low is located which will further decrease the strength of the easterly winds. This further increases the temperature of the waters, as the radiation from the sun has more time to act upon them, in the eastern Pacific as there is not the wind present to push them westward.

This feedback mechanism continues until some process prompts the system to return to a neutral or La Niña state. The mechanism for the building of a La Niña is like that of her brother, except that the pressures are reversed and the easterlies are stronger.

So, now that we have an understanding of what happens to the Pacific and the atmospheric columnar strip near the equator, how does this influence the climate of mid-latitude regions in the United States? For the most part, it is the influence that El Niño has on the mid-latitude jetstream. The mid-latitude jets are fundamentally a result of the temperature gradient between the equator and the poles. Due to differential heating of the Earth, the temperature decreases as one moves towards the poles. This creates colder, denser air as one moves towards the poles. As a result of this pressure differential, air is pulled poleward. Additionally, air is being pulled to the right in the norther hemisphere due to the Coriolis force (a product of the earth's rotation). At the latitudes where this pressure gradient force is balanced by the Coriolis force, geostrophic winds are present. However, the atmosphere at mid-latitudes across the United States, for example, is not typically *barotropic* (where the density of the air is a function of pressure only). The atmosphere is most often *baroclinic* (the density of the air is a function of pressure and temperature). This creates an environment of thermal winds. Thermal wind is a vertical shear in the geostrophic wind caused by a horizontal temperature gradient. The zonal component of the thermal wind is defined as

$$u_T = \frac{-1}{f} \frac{d}{dy} (\Phi_1 - \Phi_0) \quad (2)$$

and the meridional component is

$$v_T = \frac{-1}{f} \frac{d}{dx} (\Phi_1 - \Phi_0) \quad (3)$$

where

$$\Phi_1 - \Phi_0 \equiv gZ_T = \langle T \rangle \ln \left(\frac{P_0}{P_1} \right) \quad (4)$$

The term g is the gravitational constant, Z_T is the thickness of the layer between p_0 and p_1 measured in units of geopotential meters. So, as the change of an atmospheric layer thickness (e.g., centered at approximately 200mb) increases, so does the strength of the wind (Figure 5 shows this result for an El Niño event versus Figure 6 for a La Niña event). During an El Niño event, there is increased heating of the equatorial eastern Pacific. Thus, there is a greater temperature differential, or a larger gradient, between the tropics and the higher latitudes. As a result of this, the jetstream, which is the core of maximum zonal wind speed of the geostrophic wind resulting from thermal wind and vertical shear, is enhanced and strengthened. This provides a corridor, or pathway, where storm tracks may become more consistent. Another result of El Niño is increased water vapor that is more readily available in the warmer waters of the eastern equatorial Pacific. This is due to the fact that less energy is required to have warmer water undergo a phase change to a gas than that of cooler water. This leads to increased convection and movement of warmer and more moisture rich air to mid-latitude regions, whereby that water vapor can be precipitated out along the enhanced jetstream corridor.

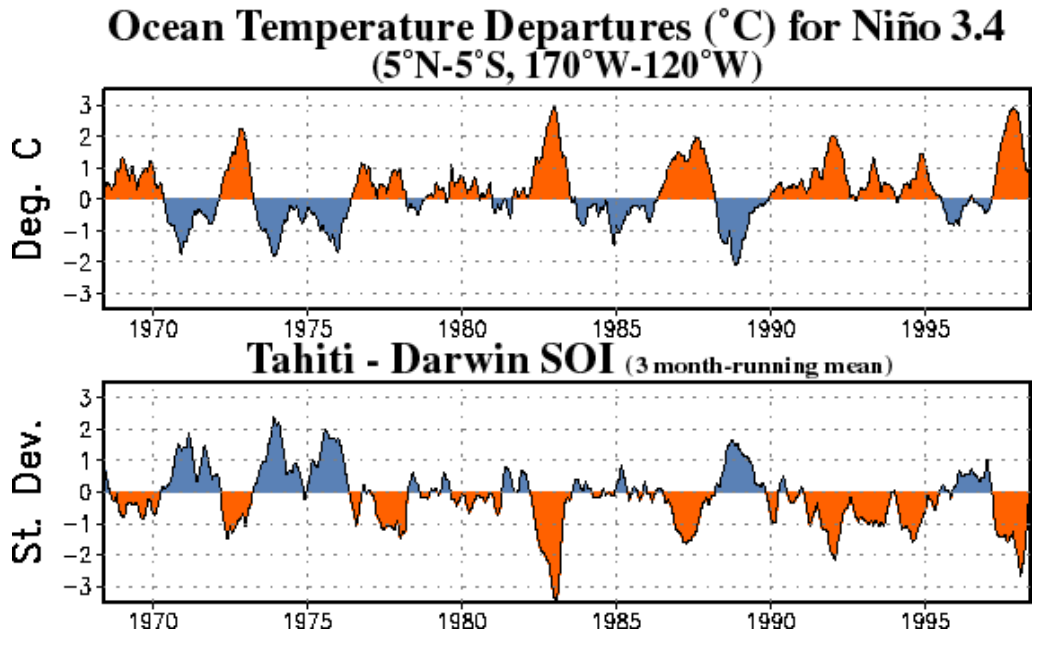


Figure 4: The relationship between the SSTs in the equatorial Pacific region NINO3.4 and the Southern Oscillation. Obtained from http://www.cpc.ncep.noaa.gov/products/analysis_monitoring/ensocycle/soi.shtml.

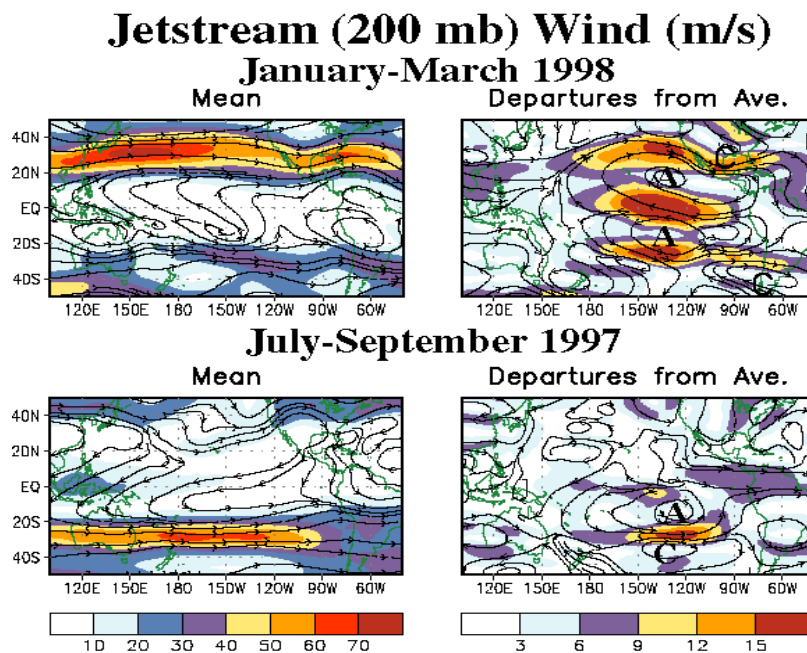


Figure 5: The winds in the jetstream during an El Niño event. Obtained from http://www.cpc.ncep.noaa.gov/products/analysis_monitoring/ensocycle/enso_circ.shtml.

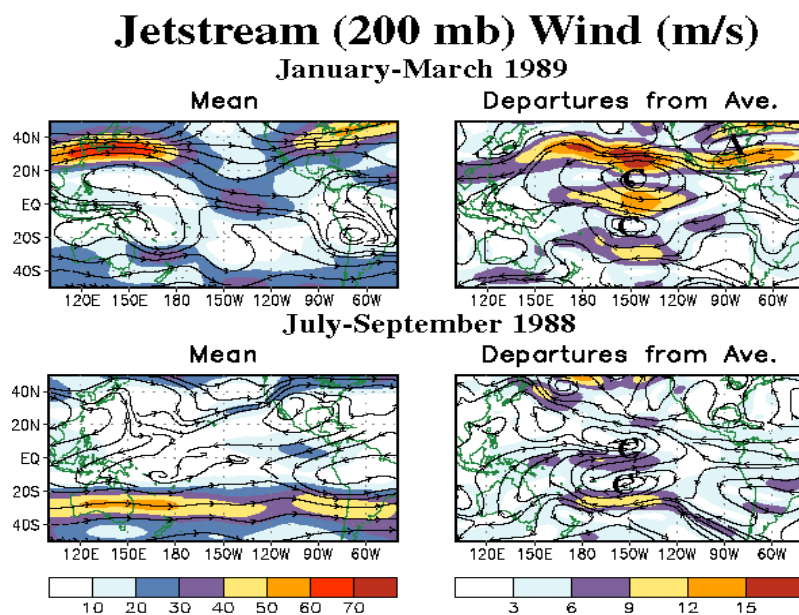


Figure 6: The winds in the jetstream during an La Niña event. Obtained from http://www.cpc.ncep.noaa.gov/products/analysis_monitoring/ensocycle/lanina_circ.shtml.

Now that the atmosphere is carrying increased water vapor in a more pronounced jetstream, this precipitable water requires delivery to the land surface. El Niño's influence is typically strongest for winter precipitation. This is due to the fact that regional winter precipitation is often the result of large-scale low pressure systems. These large-scale pressure systems are linked to occurrence of Rossby waves (Holton, 2004). Rossby waves are large, meandering planetary waves that owe their existence to the change in the Coriolis parameter ($f = 2\Omega \sin\Phi$, where Ω is the angular speed of rotation of the earth and Φ is the latitude). Rossby waves preserve absolute vorticity, which is the microscopic measure of rotation in a fluid. In the atmosphere, there is relative vorticity which is defined as

$$\zeta = \frac{\partial v}{\partial x} - \frac{\partial u}{\partial y} \quad (5)$$

and absolute vorticity,

$$\eta = \zeta + f \quad (6)$$

where f is the planetary vorticity defined earlier. Potential vorticity is defined as

$$P \equiv (\zeta + f) \left(-g \frac{\partial \theta}{\partial p} \right) = \text{Constant} \quad (7)$$

where g is the gravitational constant, θ is the potential temperature, and p is pressure. Under the constraints of the first law of thermodynamics and momentum conservation, potential vorticity is preserved (unless there is diabatic heating or frictional processes). The first term is the absolute vorticity, while the second term can be thought of as the effective depth of a vortex, which is the differential distance between potential

temperature surfaces measured in pressure units $(-\partial\theta/\partial p)$. As the depth changes, so does the vorticity. Earlier, we established that a strong El Niño provides conditions that are favorable to thermal wind at mid-latitudes, which essentially defines the rate of change of the geostrophic wind with respect to different pressure levels. However, we will confine the duration of our discussion to a constant pressure level and approximate the wind as geostrophic. Using the geostrophic momentum equations and vorticity, the local rate of change of geostrophic vorticity is given by

$$\frac{\partial \zeta_g}{\partial t} = -Vg \cdot \nabla (\zeta_g + f) + f_0 \frac{\partial w}{\partial p} \quad (8)$$

The first term on the right hand side of the equation refers to the advection of the absolute vorticity by the geostrophic wind, while the second term is the concentration or dilution of vorticity by stretching or shrinking of atmospheric fluid columns (the divergence effect). For an idealized case of mid-latitude, geostrophic flow perturbed by El Niño, we will consider the divergence to be minimal. As a result, we will neglect the second term and only consider the first term when observing El Niño's influence on the change in vorticity. So, by only considering the first term, we can rewrite equation 8 as

$$\frac{\partial \zeta_g}{\partial t} = -u_g \frac{\partial \zeta_g}{\partial x} - v_g \frac{\partial \zeta_g}{\partial y} - \beta v_g \quad (9)$$

where β is the change in the Coriolis parameter with latitude $(\partial f/\partial y)$. This equation describes the dispersion relationship for free barotropic Rossby waves. As a reminder, during an El Niño, there is lower level convergence of air due to the pressure low in the eastern equatorial Pacific. This leads to upper level divergence and as a result an increase

in southerly winds. So, as v_g increases, more negative relative vorticity is being advected in the northern hemisphere.

Assume that in our idealized case, we have a geostrophic, zonal westerly wind of 16.75 m/s at a latitude of 30N. As mentioned before, Rossby waves preserve absolute vorticity. Therefore, as air is pushed north due to the upper level divergence created by El Niño, we are advecting a decrease in relative vorticity to the air mass. In order to preserve absolute vorticity, $(\zeta+f)$, as relative vorticity is decreasing, f is proportionally increasing. This negative relative vorticity in the northern hemisphere is associated with clockwise or anti-cyclonic rotation, and thus the air will rotate clockwise and eventually begin traveling southerly again. As relative vorticity becomes equal to zero, we still have northerly flow, which will carry the air south of its original zonal track. Now, as the planetary vorticity is decreasing, relative vorticity will increase and create cyclonic curvature. As a result, the air mass will oscillate around its initial latitude. This idealized case is shown in Figure 7. It shows a closed chain of fluid particles that is perturbed, and advected relative vorticity, by the divergence of upper level air as a result of equatorial warming in the NINO3.4 domain. Rossby waves always have westward propagating phase velocity. Though, the wave's group velocity (which is associated with the energy flux) can be in any direction. Rossby's original paper (Rossby, 1939) showed that the wave's velocity to be defined as

$$c=U-\frac{\beta L^2}{4\pi^2} \quad (10)$$

where U is the mean zonal wind speed, and L is the wavelength. A negative value of c means the wave's group is traveling westward, while the wave group travels eastward with a positive c , and when c is zero, the Rossby wave group velocity is stationary with respect to the earth's surface. Returning to our idealized example, where our mean zonal wind speed is 16.75 m/s at 30N, we can rearrange equation 10 and solve for the zonal wavelength of a stationary wave using the following equation.

$$Lx = \sqrt{\frac{\bar{U} 4\pi^2}{\beta}} \quad (11)$$

Using our zonal wind speed of 16.75 m/s and our latitude of 30N, we obtain a wavelength of 5775 km, which has 6 full periods around the earth. Obviously this case is idealized and changes with the zonal wind speed and the time changing advection of relative vorticity will alter the wavelengths and the propagation speeds at varying longitudes at the same latitude. Additionally, thermal wind, divergence and convergence will all contribute to the vertical and horizontal vorticity distribution in mid-latitude meteorological systems. However, this idealized case can shed light on how El Niño conditions can induce Rossby waves that, in turn, distribute daily precipitation to regions of the United States by means of low pressure systems.

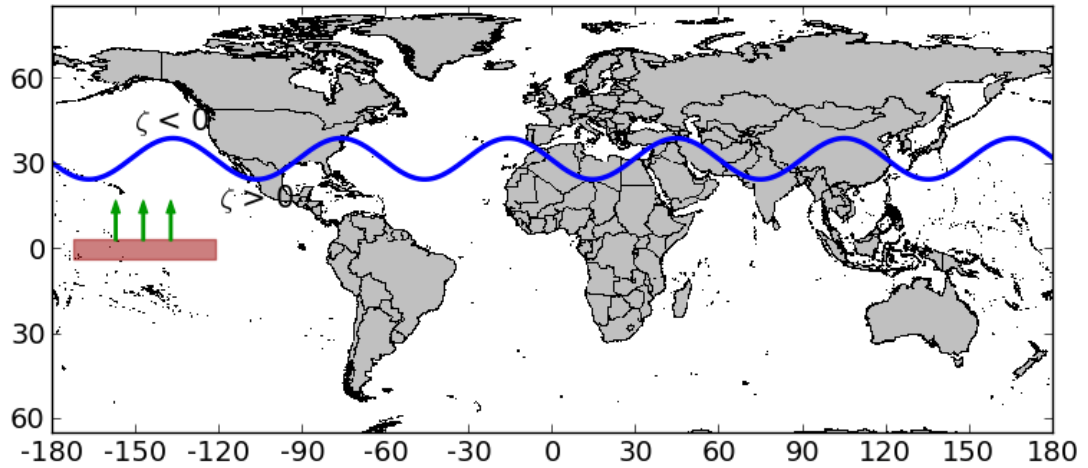


Figure 7: An idealized case of the effect of El Niño on the relative vorticity and the resulting wave pattern. This case has geostrophic flow for a closed chain of fluid particles at 30N. The resulting sinusoidal Rossby wave (blue line) is shown for some arbitrary pressure level.

The geostrophic Rossby wave example provided earlier is one manifestation of a divergence in the upper level tropical Pacific domain. These waves can be seen in the day-to-day geopotential maps. At longer time scales of months, however, a different pattern emerges that explains much of the seasonal variability. This pattern is referred to as the Pacific North American (PNA) teleconnection pattern. The PNA pattern has been shown to be a pattern of positive and negative geopotential height anomalies over the northern Pacific and North America (Horel and Wallace, 1981). The pattern appears stationary and is the result of Rossby waves that arc along a great circle. The waves start in the tropical Pacific with an anomalous and continuous heat source, proceeds northeastward, then refracts equatorward over the eastern United States. Wallace and Gutzler (1981) defined the PNA Index based on data from four points that correspond to the anomalous lows and highs of the quasi-stationary Rossby wave for the months of December-February. The PNA phenomenon is not yet clearly understood. Hoskins and Karoly (1981) proposed that the stationary train of Rossby waves resulted directly from the region of anomalous heating in the tropical Pacific. This explanation does not align with the fact the the PNA pattern is nearly the same for all El Niño episodes, though the position of anomalous heating can vary significantly between events. Another theory suggests an unstable midlatitude atmospheric mode. This mode depends on longitudinal variations of the zonal winds and can be excited by topical disturbances. General Circulation Models appear to confirm this theory, though the evidence is inconclusive. Even without a clear understanding of the PNA, it does seem to play an additional

important role in regional climate. As Philander (1990) states, “Though El Niño accounts for approximately 20% of the variance in the centers of action of the PNA pattern, it is nonetheless of importance for long-range forecasting of conditions over northern America (Namias, 1969).”

2.2 Decadal Forecasts of Colorado River Basin Streamflow

This section summarizes the methods, results and conclusions of the paper titled “Decadal Prediction of Colorado River Streamflow Anomalies Using Ocean-Atmosphere Teleconnections.” The full document is found in Appendix B.

Numerous studies have shown statistical relationships between the Atlantic Multidecadal Oscillation (AMO) and the Pacific Decadal Oscillation (PDO) to observed streamflow in the Colorado River basin. These studies were done using decadal averages of streamflow and AMO and PDO. A set of statistical relationships were shown by the authors of these studies, whereby if a given state of decadal AMO and PDO were present, one could potentially infer the current decadal streamflow quantity in the Colorado River basin. However, showing concurrent events is not always indicative of potential forecast skill. Therefore, we tested whether or not AMO and PDO could be used, statistically, to forecast Colorado streamflow for the next decade.

2.2.1 Methods and Results

Decadal averages of AMO, PDO and Colorado streamflow were first calculated. Using only past information, retrospective forecasts were made for the last 40 decadal

values of Colorado streamflow. A Euclidean distance measure (same as nearest neighbors) was used to find the closest events in the past to make retrospective forecast of 'future' events. The closest seven nearest neighbors provided the most optimal forecasts (Figure 8). Figure 9 shows the 40 retrospective decadal forecasts along with observations. The forecasted anomalies have a Nash-Sutcliffe efficiency parameter of .44 with respect to observed anomalies. These retrospective forecasts are found to be statistically significant above the 95% confidence level.

Next, reconstructions of all of the time series (derived from tree-ring statistical analysis) were used to make retrospective forecasts for a longer period of time. The forecast skills using the reconstructed AMO and PDO as predictors were only as high as the instrumental, or observed, record about 1% of the time. Lastly, we performed a frequency analysis of all of the instrumental and reconstructed data. This analysis shows that there is a dominant slower oscillating periodicity (>35yr) for all three instrumental time series (Figure 10). However, these same frequencies are not nearly as dominant or prevalent in the past.

This studies results show that there is statistically significant skill in forecasting the next decade's streamflow in the Colorado using AMO and PDO. However, the reconstructions appear to tell a different story. More observed data is required to understand how much confidence should be placed in the observed analysis. In the interim, water managers should use caution when using forecasts derived from the methodology presented in this study.

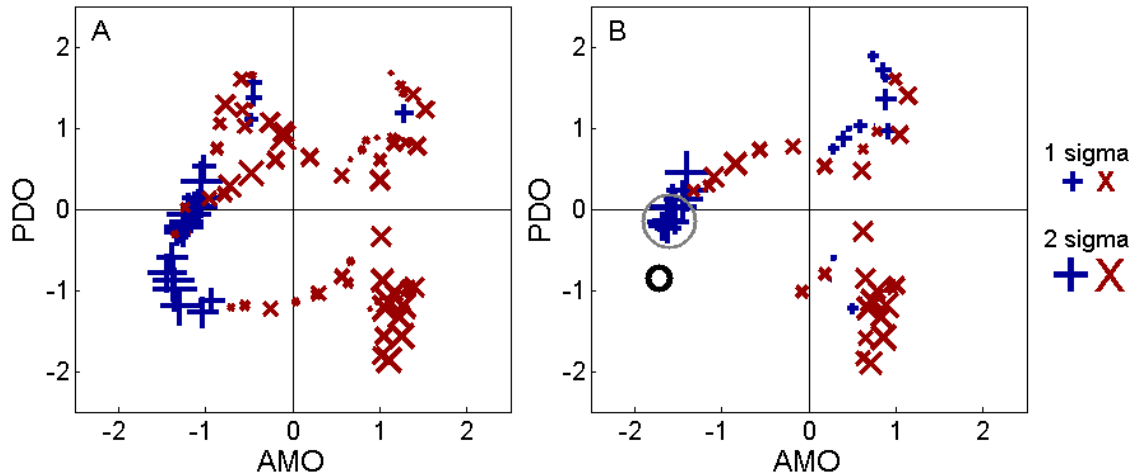


Figure 8: Plot A shows standardized departures of Lee's Ferry streamflow lagged 10 years behind departures of AMO and PDO. All values are 10-year running means. The AMO and PDO values are the 10yrRMs between 1915-1997, while the streamflows at Lee's Ferry are between 1925-2007. The + and x symbols correspond to above and below average streamflow, respectively, while the magnitudes of the departures are reflected by the size of the symbols. Plot B shows the initial 54 values (10yrRMs between 1915-1968) of AMO and PDO with Lee's Ferry streamflows lagged by 10 years. The black circle shows an example of the average AMO/PDO over the previous ten years (1978 10yrRM) that is used to predict streamflow for the following decade (1988 10yrRM). The gray circle surrounds the values that are used to make the forecast.

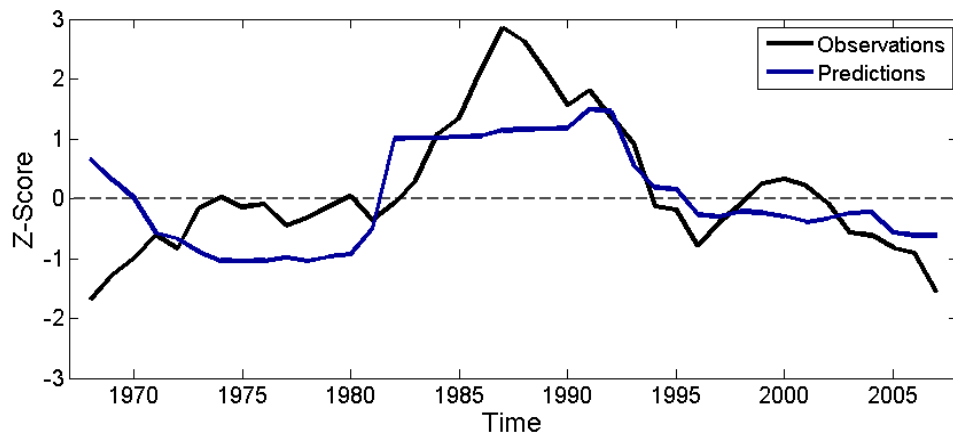


Figure 9: Observations and predictions of Lee's Ferry streamflow. The x-axis corresponds to the last year of the 10-year period of interest.

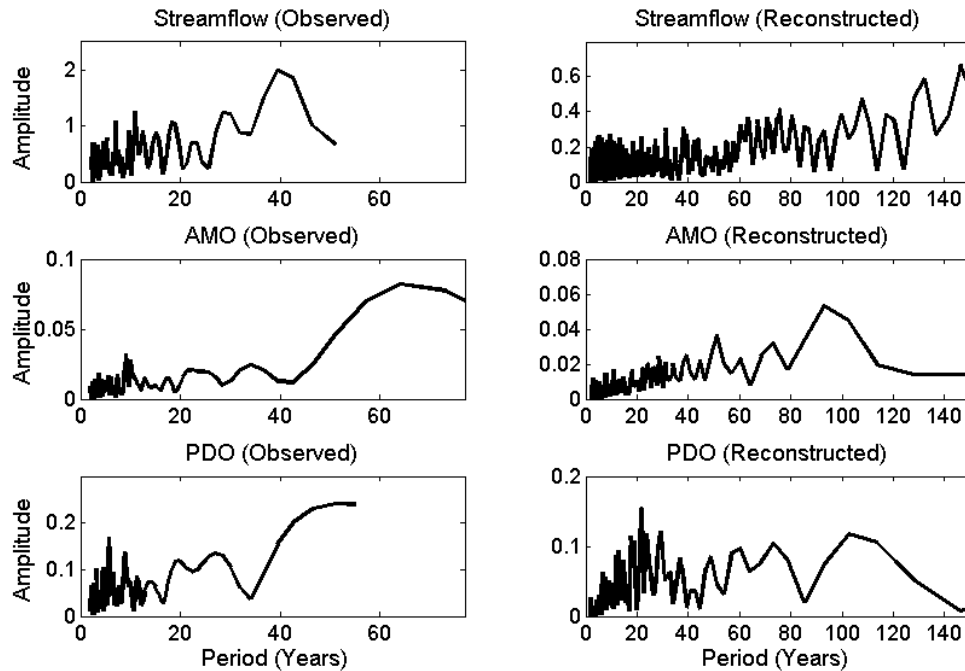


Figure 10: Frequency analyses of the observed and reconstructed records of streamflow at Lee's Ferry, AMO and PDO (reconstruction of PDO is *Biondi et al.*, 2001). The x-axes are the periods, while the y-axes are the amplitudes explained by each period. The left column all extend 77 years along the x-axis, which is half of the length of the AMO time series (statistically relevant periodicities require two cycles). There are clear dominant periods in the observed records that are seen at longer than 35 years. The reconstructed records, down the right column, do not have comparable dominant frequencies.

2.3 Expected Affects to Water Resources of the Southwestern United States Due to a Changing Climate

This section summarizes the methods, results and conclusions of the paper titled “Dynamically Downscaled and Bias-Corrected Climate Projections Exhibit a Drier Future for Southwest River Basins.” The full document is found in Appendix C.

Until recently, the computational resources were not readily available to use a Regional Climate Model (RCM) to dynamically downscale multiple global General Circulation Models (GCMs) for climate change studies. Advances in the computing field is making this a more common event, and the Department of Atmospheric Sciences at the University of Arizona has recently used the Weather Research and Forecasting model (WRF) to dynamically downscale the HadCM3 and the MPI-ECHAM5 GCMs between the periods 1968-2079 and 1950-2080, respectively. Dynamical downscaling is believed to portray more realistic future realizations than a statistical downscaling technique for two reasons. First, the model does not constrain future variable distributions by the past. And second, the model can account for complicated non-linearities that are physically based.

2.3.1 Methodology and Results

In order to obtain properly scaled projections of expected changes to the climate and the water resources of the Salt, Verde and Rio Grande river basins, our study developed an alternative bias correction methodology. The most essential difference that it has with respect to other bias correction methods, is its handling of future variability of

monthly means. A method such as Bias Correction Spatial Disaggregation (BCSD), scales future GCM monthly precipitation values by first matching it to an observed monthly time series (using its relative placement on an empirical distribution). Then, this time series is scaled by the percentage that the future GCM's monthly mean is greater or less than the long-term mean precipitation of the past GCM. However, if the ratio of the standard deviation to the mean of the GCM past is not the same as the same ratio for the observed data for the same period, then the BCSD method will inflate or deflate projected future precipitation monthly means and, as a result, the variances.

Our bias correction methodology for precipitation maps between fitted gamma distributions. We use a two parameter gamma distribution, where the mean and the variance are defined as $\alpha*\beta$ and $\alpha*\beta^2$, respectively. Therefore, it is clear that for a gamma distribution $\beta = \text{variance}/\text{mean}$ and $\alpha = \text{mean}/\beta$. We find the mean and the variance of both the gamma distributions in the time overlapping the observations and the projected time periods. The ratio by which the mean and the variance of the projected time period of the GCM differs with respect to the overlapping time period of the GCM is then multiplied by the mean and variances of the observed distribution. We then can use these new mean and variance values to solve for the α and β of a new gamma distribution. This gamma distribution will then have the same proportional shift, with reference to the observational distribution, as the shift between projected and past precipitation. Our bias correction of temperature matches the observed distribution for the past GCM time period. While the future time period first matches the observed distribution, and then each

value in the time series is offset to preserve the trends inherent to the GCM. As a result of matching this trend, both the mean and variance can shift in the future GCM with respect to observed values. Bias correction of wind speed was performed using the same methodology as for temperature. The efficacy of the bias correction is shown in Figure 11. Rows 1 and 4 of Figure 11 show the distribution parameters by time of the year (x-axis) and sorted elevation (y-axis) prior to bias correction. Rows 2 and 5 show the observed distribution parameters. Rows 3 and 6 show the distribution parameters after bias correction for the GCM past period. We can see that rows 2 and 3 and 5 and 6 are quite similar as we would expect of a successful bias correction methodology.

Now that the bias corrected HadCM3 and MPI models are more accurately simulating the seasonal climate patterns and distributions, how is the climate in these basins expected to change in the future due to the A1B (“Business as Usual”) climate change scenario? The upper row of Figure 12 shows the the percentage change in average precipitation in the projected GCM time period with respect to the past GCM time period. The x and y-axes are the same as Figure 11. The bottom two rows of Figure 12 are the differences in average maximum and minimum temperature, respectively. The HadCM3 model is projecting more precipitation in the January and June months for the time period 2011-2079 with respect to the period 1968-2010. While late April and November months are projected to be drier. The MPI model is, on average projecting a future with less precipitation (for the time period 2011-2080 with respect to the period 1950-2010). Both models are projecting, on average, between a 1°C and 3°C increase in temperature.

Changes in wind in the future time period were negligible with respect to the past period.

Figure 13 illustrates how the probability of exceedance plots change for streamflow between the projected and past GCM time periods. The blue lines show how each projected future streamflow value (expressed as a probability of exceedance on the x-axis) changes with respect to historical flows (y-axis is percentage change). The black, dotted lines are the average percentage changes in overall streamflow. For example, forcing the VIC model with HadCM3 in the Salt, approximately a 35% decrease in streamflow at 10% exceedance values (high flows) is projected for future flows with respect to what has historically been observed. Projected future climate, with both the HadCM3 and MPI models, show decreased streamflow at all values for all three basins except a slight increase at low flows in the Verde (where VIC is forced by HadCM3). The HadCM3 model is projecting on average a 23%, 20% and 22% decrease in future streamflow for the Salt, Rio Grande and Verde, respectively. The MPI model is projecting on average a 43%, 31% and 38% decrease in future streamflow for the Salt, Rio Grande and Verde, respectively. Performing a t-test for all six instances (both models for the three basins), the PJTP streamflow means were found to be statistically significantly different ($p < .01$) than the OLTP means.

To extend this research, additional GCM models can be downscaled with more climate change scenarios. This can shed light on the full distribution of projected future streamflow amounts, and provide insight as to whether these initial projections are near the median or the extremes of expected water resources under a changing climate. Also,

the RCMs could be run at a higher resolution ($<32\text{km}$), thereby better resolving certain physical processes (e.g., convective precipitation).

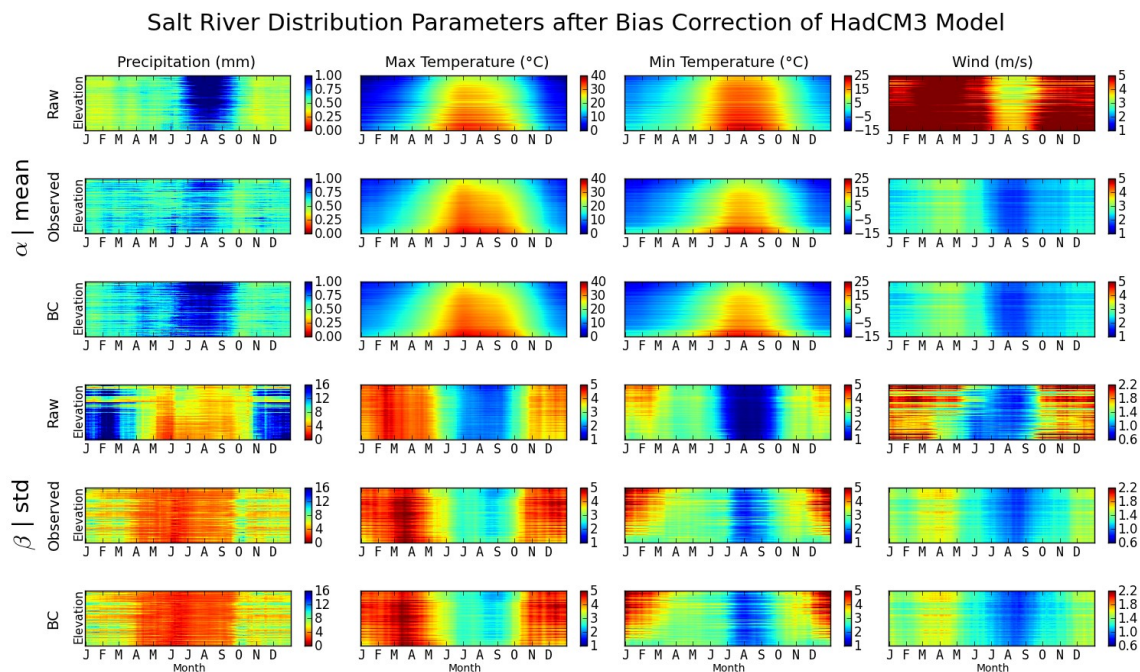


Figure 11: The raw distribution parameters α and mean correspond to the upper three rows of subplots, while β and standard deviation correspond to the bottom three rows. The first and fourth rows show the raw distribution parameters. The second and fifth rows show the observed parameters. The third and sixth rows show the bias corrected parameters. The x-axis are the days of the year with the months shown. The y-axis is sorted elevation for the Salt river, with the highest elevation on top. Ideally, if the bias corrected variable had very similar distributions to observations, rows two and three should like identical and similarly for five and six.

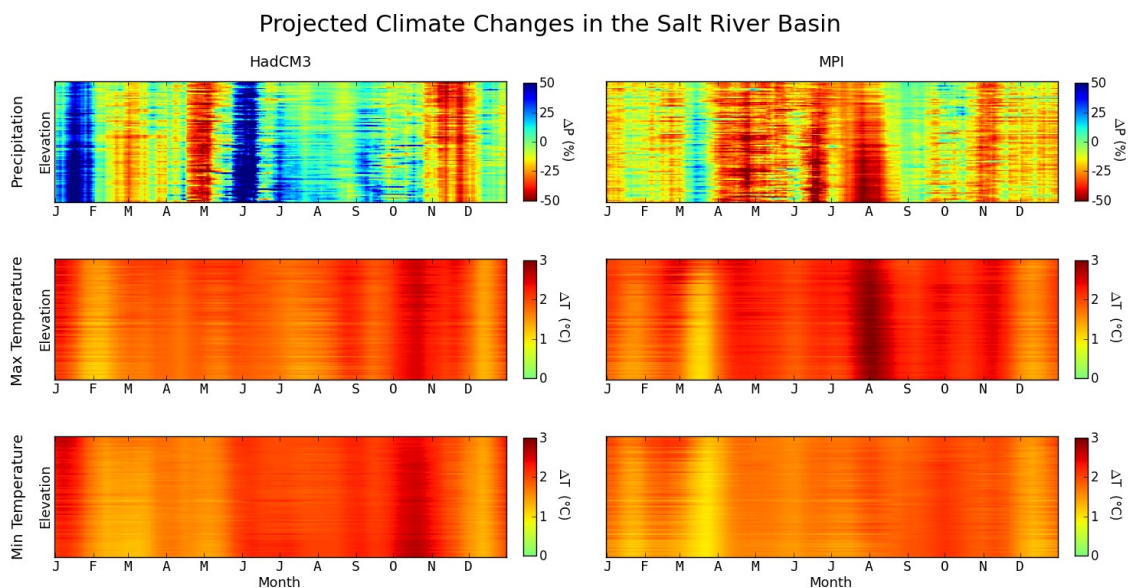


Figure 12: Projected climate changes in the Salt river basin for both the HadCM3 and MPI models. The x and y axes are same as Figure 11. The colorbars for precipitation show the percentage change in projected future values with respect to past values. The temperature colorbars show the difference between projected future values with respect to past values.

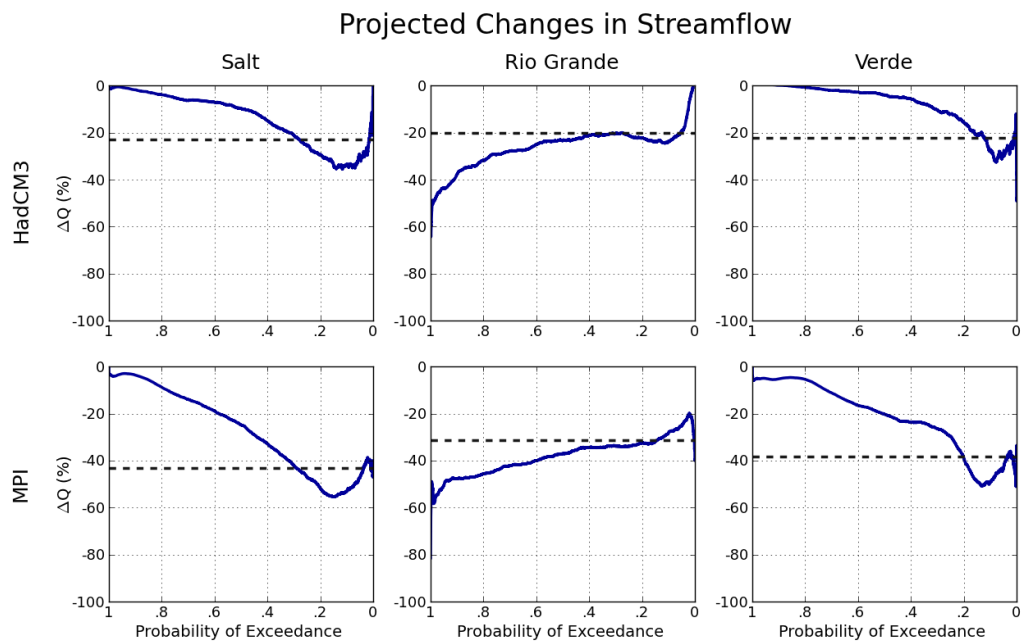


Figure 13: Projected average streamflow changes, for each probability of exceedance, in reference to the modeled data prior to the year 2011. Both models are projecting greater decreases at low flows than at high flows for the Salt and Rio Grande, while the opposite is true for the Verde.

2.4 Conclusions and Continuation of Research

Research is never completed and the stage has only been set for much more work to be done. However some progress has already been made with these studies and the results have important implications. The most relevant conclusions to my work are two-fold. First, a new benchmark in skill has been set with the proposed methodology for seasonal forecasts of precipitation. If a more complicated statistical method, or one that uses dynamical climate models, cannot exceed the average skill provided by the methodology of the first study, then why use it? This is not to say that we should be satisfied with the skill found in that study. We must always strive to improve our science. Until another method can prove that it performs better, though, we can rely on the methodology presented in the first study. Additionally, the methodology is fully objective and requires minimal resources, making it easy to implement in water stressed regions that are economically poor. The second major contribution is from the third study. This research is one of the first to use dynamical downscaling to project changes to the future climate. As a result, the projections are not constrained by the climate distributions of the past. The dynamically downscaled GCMs project decreases of approximately 25% for streamflows in select Southwest subbasins. As there are not any very substantial changes to projected future precipitation, these significant decreases are mostly the result of increasing temperatures in the region.

There are numerous areas in which the studies presented here can be extended and potentially improved. The logical next steps to be taken for the first study are as follows.

First, how much physical cohesiveness is desired in the seasonal forecasts of precipitation? We used the same parameters to forecast across the country, and we are comparing our spatially averaged skills to those of the CPC. On the other hand, different parameters could be used to optimized the forecast skill at each climate division. If this is done, we could see better skill, but there will be less emphasis on the large-scale cohesiveness of precipitation forecasts as a result of ENSO. Second, how many prior months of the ENSO index should be used and how is this related to the season? Finding an objective number of prior months that optimizes the skill for each season is necessary. Third, are there any other ENSO time series, or other teleconnections, that could be added or take the place of NINO3.4 to produce better forecast skills.

Moving on to the second study. This research proves difficult to clearly discern the next steps to be taken. The most likely next step would be to use raw sea surface temperature data (from the Extended Reconstructed Sea Surface Temperature (ERSST V3b)) to calculate an extended time series of PDO and AMO. At the same time, the tree-ring derived Lee's Ferry streamflow reconstruction can be used to extend the observed streamflow time series. This extends the predictor and predictand time series by approximately 50 years. With these time series, we can retrospectively forecast the last 100 decadal streamflow values, instead of the 40 performed in the study. Depending on how the forecast skill of the longer time series compares to that of the second study, this can help further gauge the faith one can place in the methodology.

Lastly, what are the next points of interest in continuing the third study? The

research of the third study should be replicated for additional GCM models to further expand the distribution of probable futures. Second, a temporal and spatial comparison can be made between the dynamically and statistically downscaled climate data. How similar are they, and what physical processes are most likely responsible for differences that we observe?

In many ways, my research experience has come full circle. In the beginning, my analysis of systems used a simplified approach, but perhaps the direction was wrong. With knowledge that I accrued over the years, my methodologies became increasingly more complicated. This stemmed from an incorrect assertion that the reason people have not shown improvement in something like forecasting skill, is that there is some unknown complex physical or statistical process that will yield these results. With my first two studies, in particular, I found myself reverting back to simpler methods. Furthermore, these methods weren't only computationally inexpensive, but they actually provided better results. In science, we must always weigh how much could be gained in improved skill (however it is defined) by the amount of effort required to see those improvements. Critically, this is not an argument against attempts to understand complicated physical relationships. We may not yet know how improved knowledge will be translated to the practical sciences of the future. Implementation of operational forecasts of climate and water resources, however, cannot be influenced by our emotions of what we believe to be correct or cutting-edge. Operationally, we must use the methods that have been shown to provide the best results. I find myself loving the natural sciences and the myriad of

methods that can all point to the same result. Given the many regions of the globe with significantly stressed natural resources, my hope is that our knowledge can be used most appropriately to assist us in addressing these challenges we all face.

REFERENCES

- Barnett, T. P., J. C. Adam, and D. P. Lettenmaier, 2005: Potential impacts of a warming climate on water availability in snow-dominated regions. *Nature*, **438**, 303-309.
- Bjerknes, J., 1969: Atmospheric Teleconnections from the Equatorial Pacific. *Mon. Weather Rev.*, **97** (3), 163-172.
- Christensen, N. S., A. W. Wood, N. Voisin, D. P. Lettenmaier, and R. N. Palmer, 2004: The effects of climate change on the hydrology and water resources of the Colorado river basin. *Climate Change*, **62**, 337-363.
- Held, I. M., and B. J. Soden, 2006: Robust responses of the hydrological cycle to global warming. *J. Climate*, **19**, 5686-5699.
- Holton, J. R., 2004: *An Introduction to Dynamic Meteorology*, 4th ed., Elsevier Academic Press, Burlington, 535 p.
- Horel, J. D., and J. M. Wallace, 1981: Planetary-Scale Atmospheric Phenomena Associated with the Southern Oscillation. *Mon. Weather Rev.*, **109**, 813-829.
- Hoskins, B. J. and D. J. Karoly, 1981: The steady linear response of a spherical atmosphere to thermal and orographic forcing. *Journal of Atmospheric Sciences*, **38**, 1179-1196.
- Livezey, R. E., and K. C. Mo, 1987: Tropical-Extratropical Teleconnections during the Northern Hemisphere Winter. Part II: Relationships between Monthly Mean Northern Hemisphere Circulation Patterns and Proxies for Tropical Convection. *Mon. Weather Rev.*, **115**, 3115-3132.

- McCabe G. J., and D. M. Wolock, 2007: Warming may create substantial water supply shortages in the Colorado River basin. *Geophys. Res. Lett.*, **34**, L22708, doi:10.1029/2007GL031764.
- Milly, P. C. D., J. Betancourt, M. Falkenmark, R. M. Hirsch, Z. W. Kundzewicz, D. P. Lettenmaier, and R. J. Stouffer, 2008: Stationarity is dead: whither water management? *Science*, **319**, 573-574.
- Namias, J., 1969: Seasonal interactions between the north Pacific ocean and the atmosphere during the 1960's. *Mon. Weather Rev.*, **97 (3)**, 173-192.
- O'Lenic, E. A., D. A. Unger, M. S. Halpert, and K. S. Pelman, 2008: Developments in Operational Long-Range Climate Prediction at CPC. *Weather Forecast*, **23**, 496-1044.
- Philander, S. G., 1990: *El Nino, La Nina, and the Southern Oscillation*, Academic Press, San Diego, 293 p.
- Rajagopalan, B., K. Nowak, J. Prairie, M. Hoerling, B. Harding, J. Barsugli, A. Ray, and B. Udall, 2009: Water supply risk on the Colorado River: Can management mitigate? *Water Resources Res.*, **45**, W08201, doi:10.1029/2008WR007652.
- Ropelewski, C. F., and M. S. Halpert, 1986: North American Precipitation and Temperature Patterns Associated with the El Niño/Southern Oscillation (ENSO). *Mon. Weather Rev.*, **114**, 2352-2362.
- Rossby, C. G., 1939: Relation between variations in the intensity of the zonal circulation of the atmosphere and the displacements of the semipermanent centers of action. *Journal of Marine Research*, **2 (1)**, 38-55.

Waters, M. R., and J. C. Ravesloot, 2001: Landscape change and the cultural evolution of the Hohokam along the middle Gila River and other river valleys in south-central Arizona. *Am. Antiquity*, **66** (2), 285-299.

Wallace, J. M., and D. S. Gutzler, 1981: Teleconnections in the geopotential height field during the Northern Hemisphere winter. *Monthly Weather Review*, **109**, 784-812.

APPENDIX A:

Paper was prepared to be submitted to a journal.

**An Objective and Concise Approach for Improving Seasonal Forecasts of
Precipitation Across the United States**

Matthew B. Switanek¹, Peter A. Troch²

¹Hydrology and Water Resources, University of Arizona

1133 E James E. Rogers Way Rm. 320A,

Tucson, AZ 85721

²Hydrology and Water Resources, University of Arizona

1133 E James E. Rogers Way Rm. 320,

Tucson, AZ 85721

ABSTRACT

An objective and concise methodology is proposed to improve the forecasts of seasonal precipitation. The method uses a combination of a linear model and a nearest neighbors model. Both of these models use only the most recent 1 month or 3 month average of the NINO3.4 index as a predictor. Using a fixed model, we find improvement in the spatially averaged skill over the CPC for all seasons except for ASO.

1. Introduction

There is an abundance of water resources across the United States. Unfortunately, these resources are not very uniformly distributed. Regions such as the Southwest, where the Colorado River resides, have long ago fully allocated its available surface water. Improving near-term climate forecasting is essential to help alleviate the challenging and complex decisions that lawmakers and water managers face across the country (Becker et al., 2013; Shukla et al., 2013).

The Climate Prediction Center is under the umbrella of the National Weather Service, and is responsible for making seasonal forecasts of climate across the United States (O'Lenic et al., 2008). These forecasts are made for three month seasons at lead times of between 1 and 13 months. They use a variety of statistical and dynamical methods to assist in making their forecasts. Over time, they have attempted to move away from subjective discussions of expected climate to an objective methodology. They rely heavily on the El Niño Southern Oscillation (ENSO) phenomenon to make their forecasts

(Bjerknes, 1969; Castro et al., 2001; Goddard et al., 2001; Higgins et al., 2000, Horel and Wallace, 1981; Mason and Goddard, 2001; McCabe and Dettinger, 2002; Ropelewski and Halpert, 1986) .

We began our study skeptical of the power of ENSO to be used so broadly for seasonal climate forecasting. More specifically, we did not believe that ENSO had a stronger and more robust relationship to precipitation, on average across the United States, than any other combination of time series. With much effort, we could find no other index, or combination thereof, that came close to providing the overall level of skill as ENSO.

This study focuses on whether or not an objective and concise methodology can be developed to improve upon the forecasts made by the CPC. This study uses a test case of near-term forecasts (the next season) of precipitation across the US. We investigate the skill levels of moderately simple models that use NINO3.4 as a predictor and compare these skills to archived forecasts of the CPC.

2. Data and Methodology

a. Data and Study Location

The Extended Reconstructed Sea Surface Temperature (ERSST V3b) was used to calculate the monthly NINO3.4 time series between the time period of 1901-2012, where NINO3.4 is defined as the average SSTs between 120°W-170°W and 5°S-5°N. This time series was very highly correlated with the NINO3.4 used by the CPC

(<http://www.esrl.noaa.gov/psd/data/correlation/nina34.data>) with a correlation coefficient greater than .99 for the time period 1950-2012. We therefore assume that our calculated NINO3.4 is representative of the phenomenon prior to 1950. Monthly precipitation data across the contiguous US was obtained from the PRISM group (PRISM Climate Group, Oregon State University, <http://prism.oregonstate.edu>) for the time period 1901-2012.

Archived forecasts of precipitation, made by the CPC, were obtained from their website at <http://www.cpc.ncep.noaa.gov/pacdir/NFORdir/HUGEdir2/hut.html>. This page has archived probabilistic forecasts of precipitation at lead times of 1 to 13 months. We used the data between the years 1994-2011 which correspond to forecasts made for the seasons JFM, 1995 through JFM, 2012. In this time period with a lead time of 1 month, there have been 18 forecasts for the JFM season and 17 forecasts for the other 11 seasons. Since the variances of the CPC's and our forecasts are typically not very different from the climatological variance, changes in probabilistic skills is most reflective of forecasted means. Therefore, we chose to use a deterministic skill measure, that uses the most likely forecasted values (50th percentile), to compare forecast success. The skill measure that we use is defined as

$$\text{Skill} = r * (1 - (1 - CV)^2) \quad (1)$$

where r is the correlation coefficient between the forecasted and observed values, and CV is the ratio of the coefficient of variations of the forecasted to the observed values. This measure of skill ensures that forecasts have both a positive correlation and represent a reasonable level of variability with respect to observations. Forecasts that are highly

correlated, but represent little variability are not very useful, and thus are penalized as such. Values less than zero can be interpreted to have no skill. In these locations, it is better to use the climatological value of precipitation than the forecasted values. Values greater than zero have performed better than the climatology in the past, and have the potential to do so in the future. A value of 1 would be perfectly correlated, with a complete alignment of the variabilities. Bias is not considered in this study, though we found there to be no consistently strong biases by either the CPC or our forecasts.

b. An Objective and Concise Forecasting Methodology

For our study, each model only uses NINO3.4 as a predictor. The model makes forecasts that are comprised of two separate methodologies. These are a simple linear regression, which minimizes ordinary least squares, and a nearest neighbors algorithm. The following sections provide an outline of the independent models in addition to the proposed methodology which combines two of the models in a specified manner.

1) LINEAR MODEL USING CLIMATOLOGY

The linear relationship between NINO3.4 and precipitation, for the past 30 years, across the country was used to forecast precipitation for the next season. For example, a linear regression line was fit between NINO3.4 and precipitation for a specified climate division and season. This model is subsequently referred to as LM-C3M (Linear Model using the Climatological values of the most recent average 3 Months of NINO3.4). To further illustrate, the average September-November (SON) NINO3.4 values were used as

predictors for the precipitation in the following January-March (JFM) season for climate division 1. Data for the years 1965-1994 were used to train the model, then a retrospective forecast was made for the JFM 1995. Retrospective forecasts were made, only with the use of past data, for the years 1995 through 2012.

2) LINEAR MODEL USING EXTENDED TIME SERIES

This model fits a linear regression to all the years prior to the year we are making a forecast. For example, to forecast the JFM 1995 precipitation, the model would first linearly fit the NINO3.4 and precipitation data for the time period 1901-1994. Then, the fit model is used with the 'current' SON NINO3.4 value in 1994 to make a forecast of JFM 1995 precipitation. This model is subsequently referred to as LM-AP3M (Linear Model using All Prior values of the most recent average 3 Months of NINO3.4). The same procedure is performed for all seasons.

A linear model that that is identical to the LM-AP3M is used except that the past 1 month average NINO3.4 is the predictor instead of the past 3 month average. This model is subsequently referred to as LM-AP1M.

3) NEAREST NEIGHBORS MODEL USING EXTENDED TIME SERIES

This model fits a set of nearest neighbors to past data. Similarly to the linear model, the skills were greater when considering the extended time series. We will, therefore, focus on the forecasts obtained using the extended NINO3.4 time series as a predictor. Both the past season and the past month of NINO3.4 were implemented. These models are hereafter referred to as NNM-AP3M and NNM-AP1M (Nearest Neighbors

Model using All Prior values of the most recent average 3 Months and 1 Month of NINO3.4, respectively). Initially, forecasts of precipitation were made using different numbers of the closest nearest neighbors. For example, the closest distance between the most recent NINO3.4 value to a past NINO3.4 value is found, and the precipitation that seasonally follows that past NINO3.4 value is used as the forecast. Next, increasing numbers of nearest neighbors were used, so that the forecasts were the average of multiple precipitation values that were closest, in data space, to past events. A set of forecasts using nearest neighbors 1 through 8 were obtained.

There is now a set of time series of potential forecasts, for the NNM-AP3M and NNM-AP1M, where each time series is for the period 1971-2012 and using nearest neighbors 1 through 8. Which of these sets, progressing forward in time, will have provided the best skills in the past? To be true to the difficulties that CPC faces at the time, no future information was used to overfit the level of skill. For example, to make a JFM 1995 precipitation forecast for climate division 1, the time series of forecasts that provided the best skills between 1971-1994 are used. This is done by simply finding which sets of nearest neighbor forecasts had provided positive skill for the time period 1971-1994. If that happened to correspond to nearest neighbors 3, 4 and 5, then it is those three forecasts that are equally weighted to make a forecast for the JFM season in 1995. Then to make a forecast for JFM 1996, the skills from the time period 1971-1995 is considered.

4) COMBINED LINEAR AND NEAREST NEIGHBORS MODEL USING THE

EXTENDED TIME SERIES

Lastly, our final forecasts are obtained by equally weighting the forecasts from both the LM-AP1M and NNM-AP1M. The methodology put forth is only a first order attempt to make improvements in the skill level of near-season precipitation forecasts. So, all potential parameters that could be changed or adjusted were held constant. In the Discussion and Conclusions section, we discuss some of the potential paths one could take to further improve skill.

3. Results

a. Forecasting Skill of the Climate Prediction Center

The CPC's next season precipitation forecast skills are seen in Figure 1. Cooler colors represent higher skill, while everything that is not completely red represents some amount of skill. The regions of saturated red show that, up to date, there is no discernible forecast skill in these regions for these seasons. For the regions of red, one should probably use the climatological mean precipitation for next season forecasts instead of CPC's forecasts. It is clearly visible that there is the most skill along the southern tier of the US during the winter months. In the spring through the fall, most of the country has little to no forecast skill.

b. Forecasting Skill of the Climatological Linear Model

The forecast skills of the linear, climatological model in contrast to the CPC's is shown in Figure 2. The blue scatter points correspond to the skill of the CPC (x-axis)

versus the skill of the linear, climatological model (y-axis). There are 102 blue scatter points representing the 102 climate divisions. Values above the one-to-one line show climate divisions that have higher skill using the linear, climatological model. Values below the line show the climate divisions that the CPC has more skill forecasting. The improved number of climate divisions (ICD), using the linear model, is listed in the lower right of each subplot for each season. The larger red scatter point shows the spatially averaged means for that particular season. Again, if the red scatter point is above the line, then the linear model is doing better, on average for that season, in forecasting precipitation. The green point is the average of the skills that are positive. If there is some persistence in the spatial distribution and strength of the skills, then this has meaning. For example, if one has some reason to believe that regions which have some skill now will have similar skill in the future, then the green scatter point shows how much better or worse the linear positive skills are with respect to the CPC's positive skills (these are not necessarily the same climate divisions). We observe that spatially averaged skills are better, when simply using a linear model of the past 30 years, for the seasons DJF, JFM, FMA, MAM, OND, and NDJ. While the CPC's forecasts have better spatially averaged skills for the other seasons. If, however, we believe that regions with skill now may continue to have skill, then it can be seen that the green scatter points are always above the one-to-one line. Therefore, climate divisions that have positive skill have a higher average value, using the linear climatological model, than the CPC's climate divisions with positive skills.

c. Forecasting Skill of the Linear Model Using the Extended Time Series

The forecast skills of the linear model, using the extended time series, are shown in contrast to the CPC's skills in Figure 3. The red scatter points now show that the forecasts using this linear model are better, on a spatial average, than the archived CPC skills for each season through the year. Again, the skills using this model are also higher when averaging the positive skills (green scatter points).

There continue to be some modest improvements when using only the most recent month's NINO3.4 instead of the most recent 3 months. These results are not shown across space, but they are summed up as spatially averaged skills through time in Figure 8, which is discussed in more detail to come.

d. Forecasting Skill of the Nearest Neighbors Model Using the Extended Time Series

The forecasts using a nearest neighbor model adds improvements for many climate divisions in the winter seasons, and for some climate divisions during other seasons. The model is not as conservative in its approach, and therefore the worst skills with this model are worse than using the linear model. If one considers that regions that are skillful now, will also be so in the future, then the nearest neighbors model adds a substantial amount of skill. This is made clear when combining this model with that of the linear model.

e. Forecasting Skill of the Combined Linear and Nearest Neighbors Model Using the Extended Time Series

Figure 4 shows the spatial distribution of forecast skill by season. Here, the

combined forecasts of the linear and nearest neighbor models is implemented using the most recent completed month of NINO3.4. Comparing Figure 4 to Figure 1, it is apparent that when using the proposed methodology herein, substantial improvements are made in forecasting precipitation across large areas of the US. Figure 5 shows the skills in Figure 4 minus the skills in Figure 1. The cooler colors in Figure 5 show the season and the regions where the proposed methodology is forecasting more skillfully, while the warmer colors show where and when the CPC has historically had more skill. Figure 6 presents the DJF precipitation forecasts for climate division 98 using the 50th percentile values from our proposed methodology (blue scatter points) versus the CPC (green scatter points). This is an example where the CPC's forecast is already skillful with a value of .27 (with $r = .53$, $CV = .3$), while we observe some improvement with a skill of .52 (with $r = .84$, $CV = .38$) using the most recent month's NINO3.4 in the combined linear and nearest neighbors model. Figure 7 is the same as Figures 2 and 3, but for the combined model. The combined model's results provide the best overall results, with making improvements in forecast skill in seasons throughout the year, and in particular during the winter time. However, the season of ASO is performing worse, on average (red scatter point), than the CPC's forecasts. While other seasons see a modest improvement in overall skill. The green scatter points show that, when using the proposed methodology, the regions with positive skill are more skillful than those of the CPC.

The spatially averaged skills across the US for each of the seasons, using the different methodologies, is shown in Figure 8. The CPC's average skills, by season are

shown in black, while the climatological linear model that uses NINO3.4 as a predictor is the gray line. Additionally, the red and green lines are the linear models using all prior values of 3 and 1 month averaged NINO3.4 and precipitation, respectively. Finally, the blue line is the resulting forecasts that incorporated both the LM-AP1M and the NNM-AP1M models. It can be observed that only using NINO3.4 as a predictor in a linear model (all years prior, either 3 or 1 month average NINO3.4), there is more skill, on average, than historic CPC forecasts of near season precipitation.

4. Discussion and Conclusions

It is interesting to note that the level of skill, averaged over space for each of the seasons of the year (with the exception of ASO), is as good or exceeds the CPC's skill. The CPC has multiple tools at its disposal to make forecasts, but they appear to not add any skill above and beyond using a linear model with one predictor. Given its simplicity, this model should be used to provide an objective baseline that is similar to that of the CPC. By additionally adding in the forecasts of a nearest neighbors model, we see further overall improvement in the skill.

The results have shown the forecasts made by a combined model that had no changing parameters, and thus may not be performing as well in some seasons or for some climate divisions as possible. However, if the model is catered more specifically to a particular season, we can potentially observe further improvements. Consider the forecasts made for the season ASO, in which our model performed worse than the CPC.

For this season, if we use a combined model of LM-AP3M and NNM-AP3M instead of the combined LM-AP1M and NNM-AP1M, we improve our average spatial skill from $-.012$ to $.048$. Figure 9 shows the differences in the ASO forecasts when using the combined model and just the prior month's NINO3.4 (top subplot) versus the prior three month's NINO3.4 (bottom subplot). The overall level of skill substantially increases. This is curious, as this is not the case with forecasts of, for instance, DJF. Therefore, maybe this could tell us something about relevant ocean/atmosphere frequencies in different seasons of the year. Possible next steps one could take to further improve on the current study are as follows. First, one could optimize model forecast skill as a spatial average, which in that case seems to rely on some cohesive physical mechanism controlling seasonal precipitation. Otherwise, the forecast skill could be optimized for each individual climate division. Second, additional predictors can be added to the model. These predictors could be different past months of NINO3.4 that have a greater lead time, or perhaps the Pacific Decadal Oscillation index.

As it stands, seasonal forecasting of precipitation may not need to be so complicated. That is if our goal is to match or slightly exceed current forecast skill. It appears as though there is more predictive information, pertaining to climate, in ENSO than has been commonly used. Taking advantage of different methods that use the entire records of these time series can be invaluable in further increasing forecast skill. These subtle changes in a simpler statistical forecast model could even lead to a greater physical understanding of our climate system.

References

- Barnston, A., 1994: Linear Statistical Short-term Climate Predictive Skill in the Northern Hemisphere. *J. Climate*, **7**, 1513-1564.
- Becker, E. J., H. Van Den Dool, and M. Peña, 2013: Short-Term Climate Extremes: Prediction Skill and Predictability. *J. Climate*, **26**, 512-531.
- Bjerknes, J., 1969: Atmospheric Teleconnections from the Equatorial Pacific. *Mon. Weather Rev.*, **97** (3), 163-172.
- Castro, C. L., T. B. McKee, and R. A. Pielke Sr., 2001: The Relationship of the North American Monsoon to Tropical and North Pacific Sea Surface Temperatures as Revealed by Observational Analyses. *J. Climate*, **14**, 4449-4473.
- Goddard, L., S. J. Mason, S. E. Zebiak, C. F. Ropelewski, R. Basher, and M. A. Cane, 2001: Current Approaches to Seasonal-to-Interannual Climate Predictions. *Int. J. Climatol.*, **21**, 1111-1152.
- Higgins, R. W., A. Leetmaa, Y. Xue, and A. Barnston, 2000: Dominant Factors Influencing the Seasonal Predictability of U.S. Precipitation and Surface Air Temperature. *J. Climate*, **13**, 3994-4017.
- Horel, J. D., and J. M. Wallace, 1981: Planetary-Scale Atmospheric Phenomena Associated with the Southern Oscillation. *Mon. Weather Rev.*, **109**, 813-829.
- Livezey, R. E., and K. C. Mo, 1987: Tropical-Extratropical Teleconnections during the Northern Hemisphere Winter. Part II: Relationships between Monthly Mean Northern

- Hemisphere Circulation Patterns and Proxies for Tropical Convection. *Mon. Weather Rev.*, **115**, 3115-3132.
- Mason, S. J., and L. Goddard, 2001: Probabilistic Precipitation Anomalies Associated with ENSO. *B. Am. Meteorol. Soc.*, **82** (4), 619-638.
- McCabe, G. J., and M. D. Dettinger, 1999: Decadal Variations in the Strength of ENSO Teleconnections with Precipitation in the Western United States. *Int. J. Climatol.*, **19**, 1399-1410.
- McCabe, G. J., and M. D. Dettinger, 2002: Primary Modes and Predictability of Year-to-Year Snowpack Variations in the Western United States from Teleconnections with Pacific Ocean Climate. *J. Hydrometeorol.*, **3**, 13-25.
- O'Lenic, E. A., D. A. Unger, M. S. Halpert, and K. S. Pelman, 2008: Developments in Operational Long-Range Climate Prediction at CPC. *Weather Forecast*, **23**, 496-1044.
- Ropelewski, C. F., and M. S. Halpert, 1986: North American Precipitation and Temperature Patterns Associated with the El Niño/Southern Oscillation (ENSO). *Mon. Weather Rev.*, **114**, 2352-2362.
- Shukla, S., J. Sheffield, E. F. Wood, and D. P. Lettenmaier, 2013: On the Sources of Global Land Surface Hydrologic Predictability. *Hydrol. Earth Syst. Sci. Discuss.*, **10**, 1987-2013.

Figures

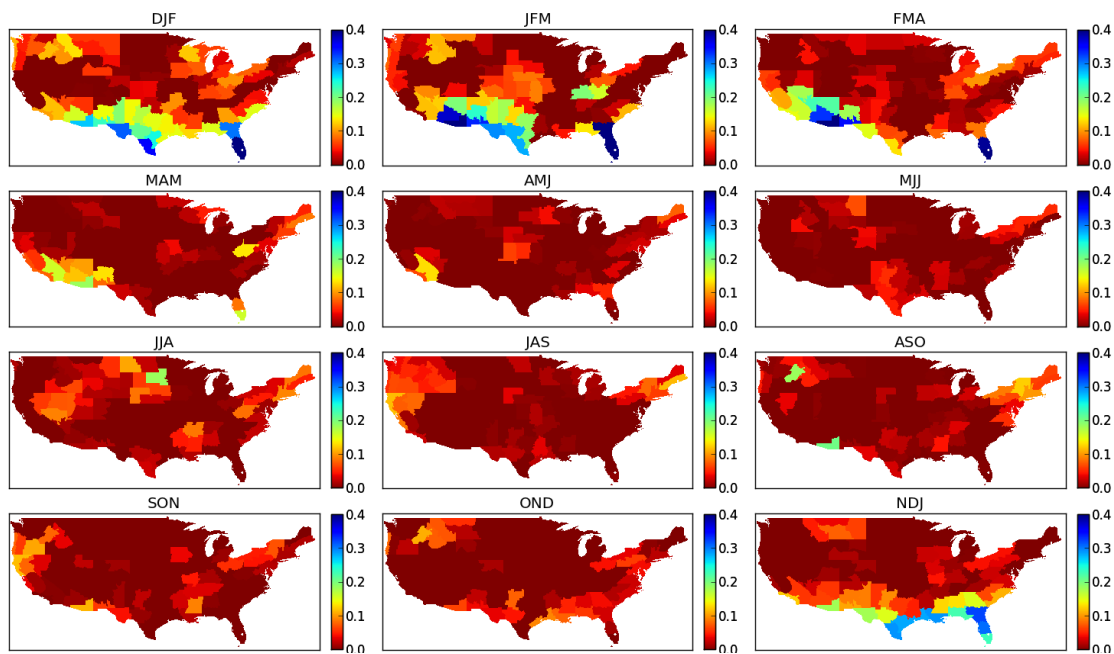


Figure 1: The CPC's next season precipitation forecast skills. Cooler colors represent higher skill, while everything that is not completely red represents some amount of skill. The regions of saturated red show that, up to date, there is no discernible forecast skill in these regions for these seasons.

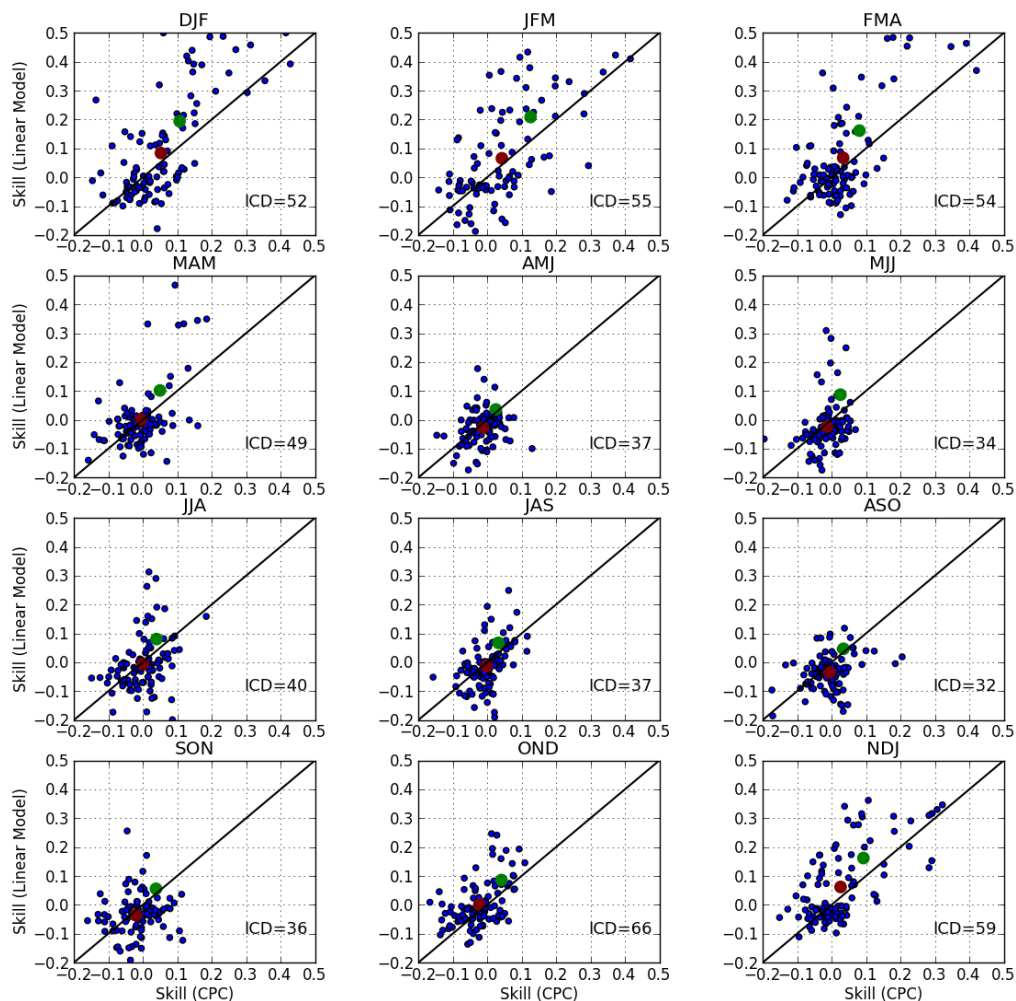


Figure 2: The forecast skills of the linear, climatological model in contrast to the CPC's. The blue scatter points correspond to the skill of the CPC (x-axis) versus the skill of the linear, climatological model (y-axis). There are 102 blue scatter points representing the 102 climate divisions. Values above the one-to-one line show climate divisions that have higher skill using the linear, climatological model. Values below the line show the climate divisions that the CPC has more skill forecasting. The improved number of climate divisions (ICD), using the linear model, is listed in the lower right of each subplot for each season. The larger red scatter point shows the spatially averaged means for that particular season. The green point is the average of the skills that are positive.

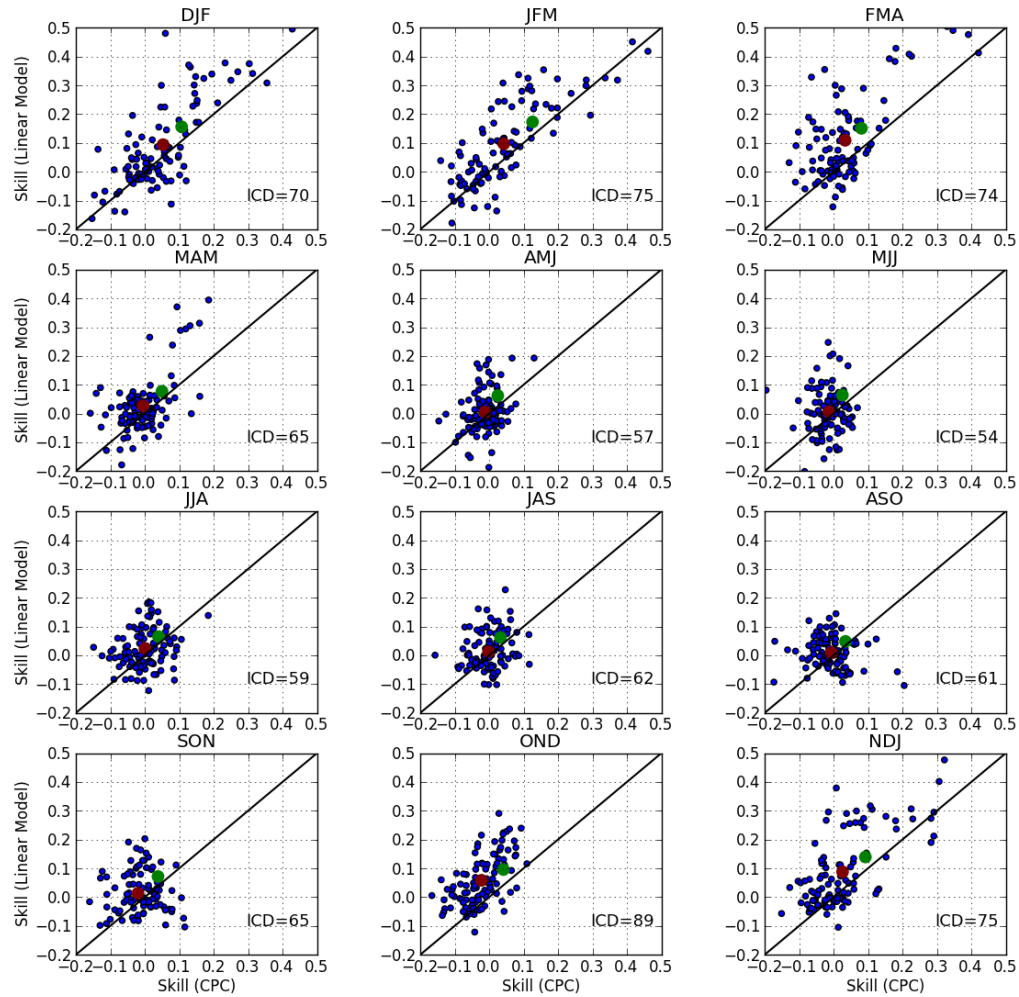


Figure 3: Same as Figure 2, except the forecast skills are for the linear model, using the extended time series, in contrast to the CPC's skills.

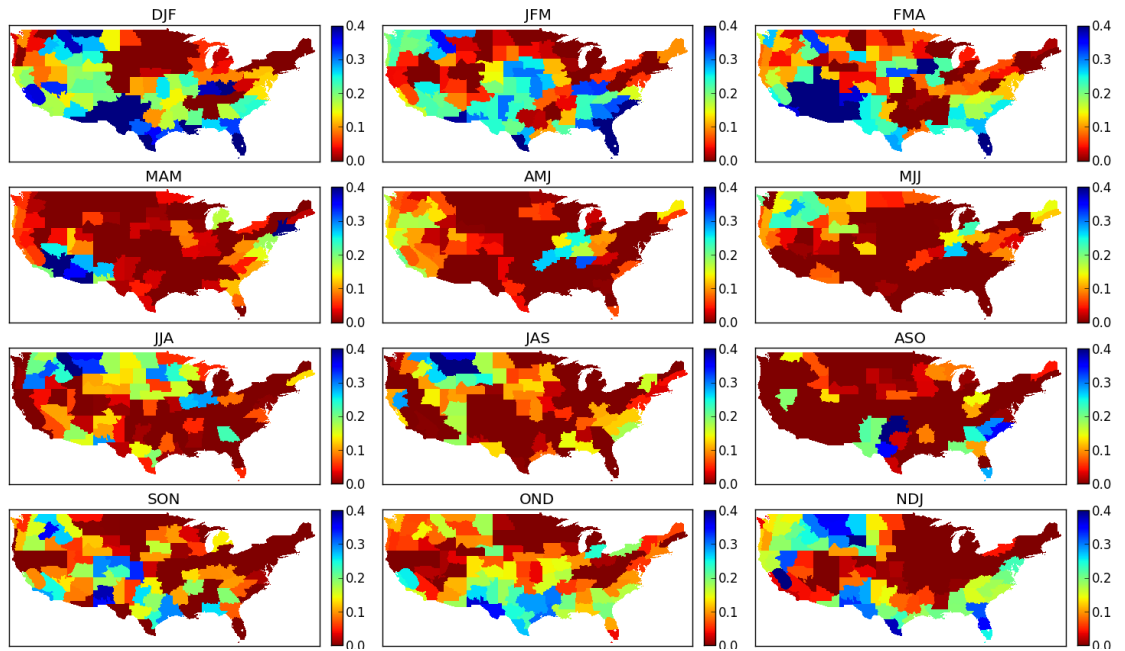


Figure 4: The spatial distribution of forecast skill by season. Here, the combined forecasts of the linear and nearest neighbor models is implemented using the most recent completed month of NINO3.4.

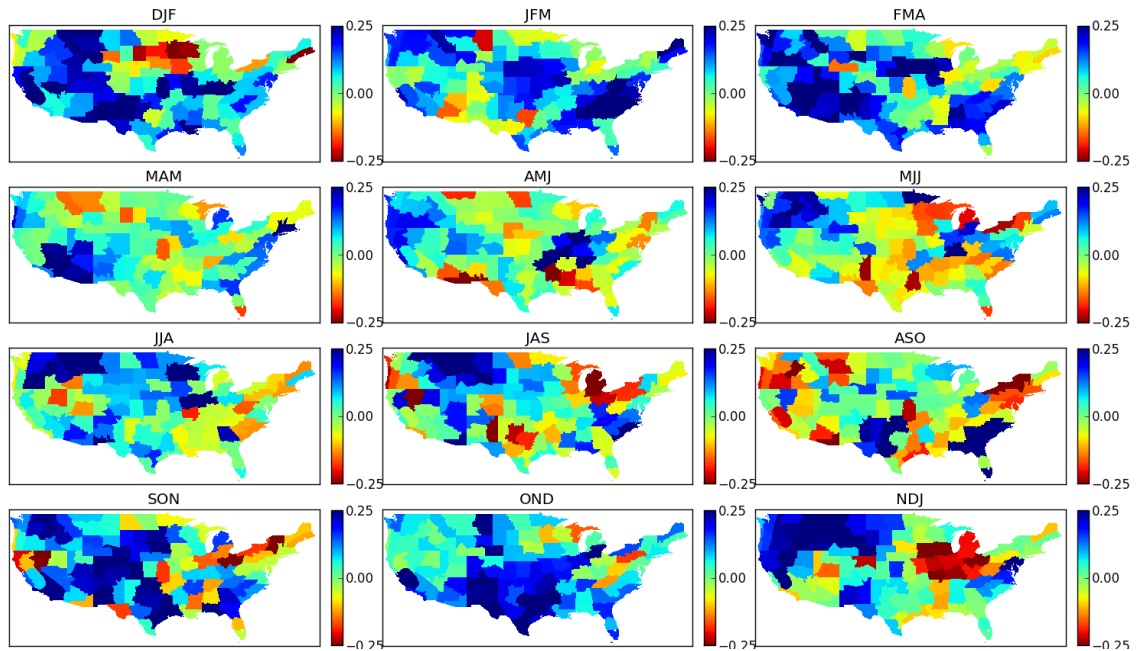


Figure 5: The difference between Figure 4 and Figure 1. Cool and warm colors are regions where our proposed methodology is performing better and worse than the CPC, respectively.

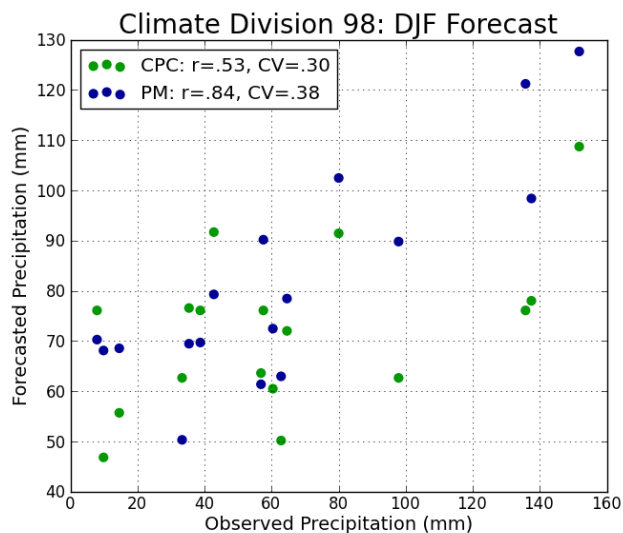


Figure 6: The DJF precipitation forecasts for climate division 98 using the 50th percentile values from our proposed methodology (blue scatter points) versus the CPC (green scatter points). This is an example where the CPC's forecast is already skillful with a value of .27 (with $r = .53$, $CV = .3$), while we observe some improvement with a skill of .52 (with $r = .84$, $CV = .38$) using the most recent month's NINO3.4 in the combined linear and nearest neighbors model.

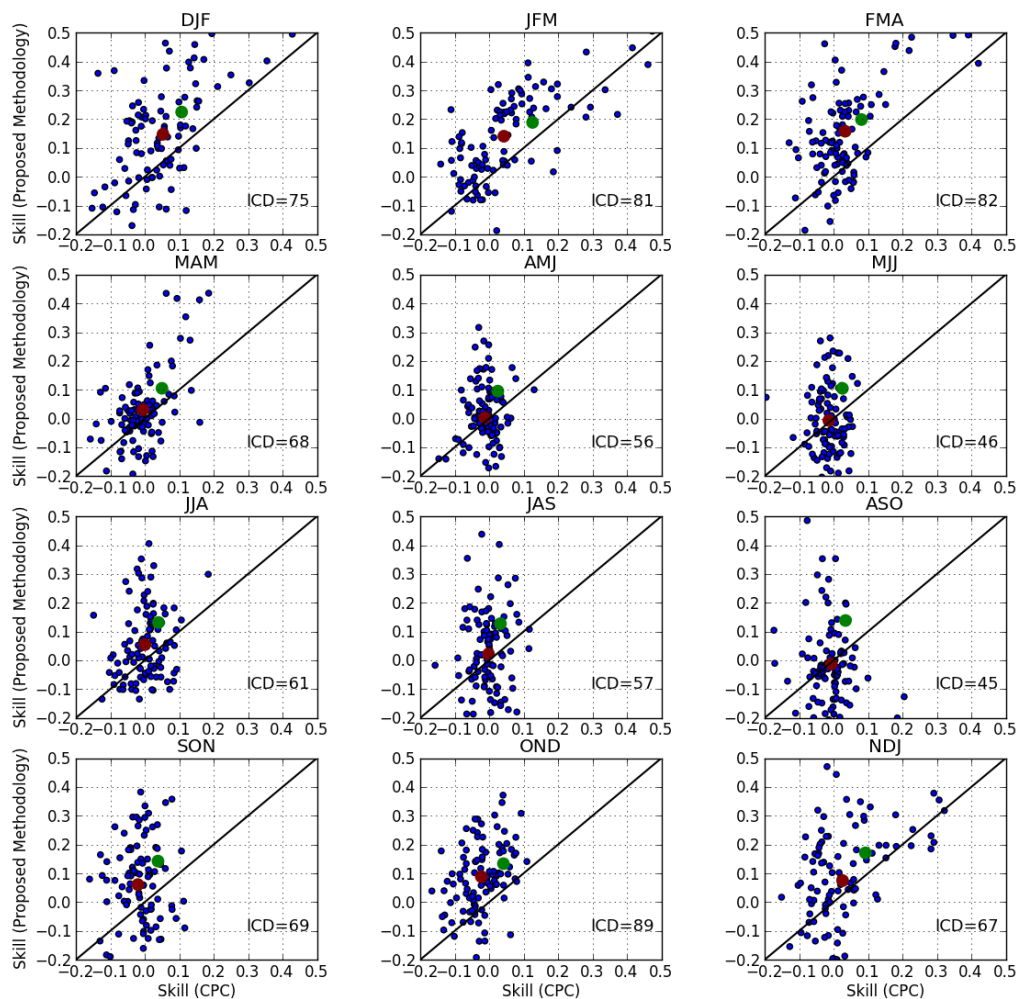


Figure 7: The same as Figures 2 and 3, but for the combined model. The combined model's results provide the best overall results, with making improvements in forecast skill in seasons throughout the year, and in particular during the winter time.

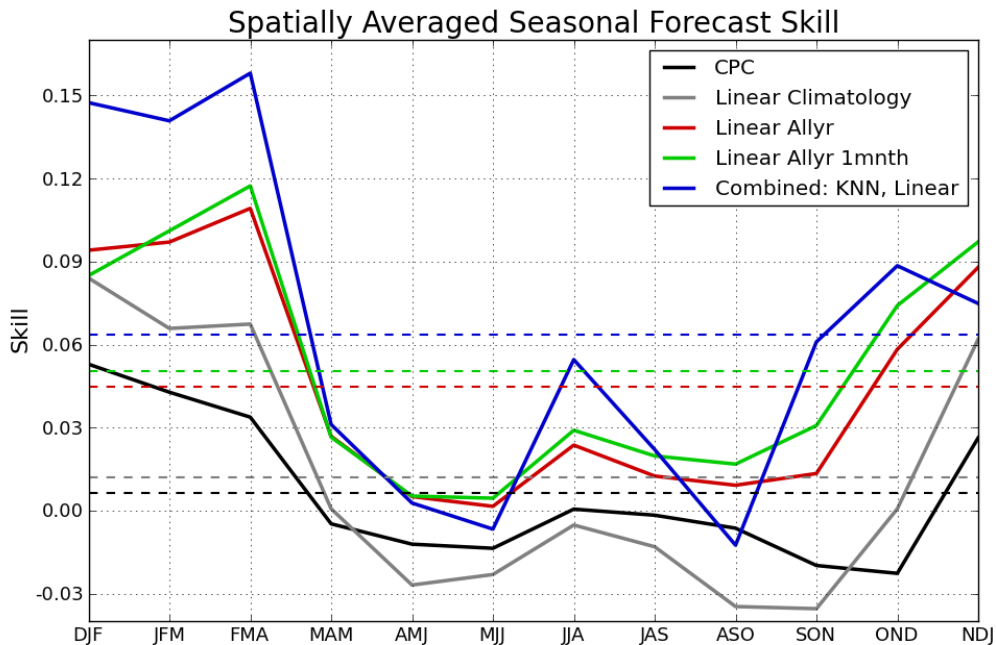


Figure 8: The CPC's average skills, by season are shown in black, while the climatological linear model that uses NINO3.4 as a predictor is the gray line. The red and green lines are the linear models using all prior values of 3 and 1 month averaged NINO3.4 and precipitation, respectively. The blue line is the resulting forecasts that incorporated both the LM-AP1M and the NNM-AP1M models.

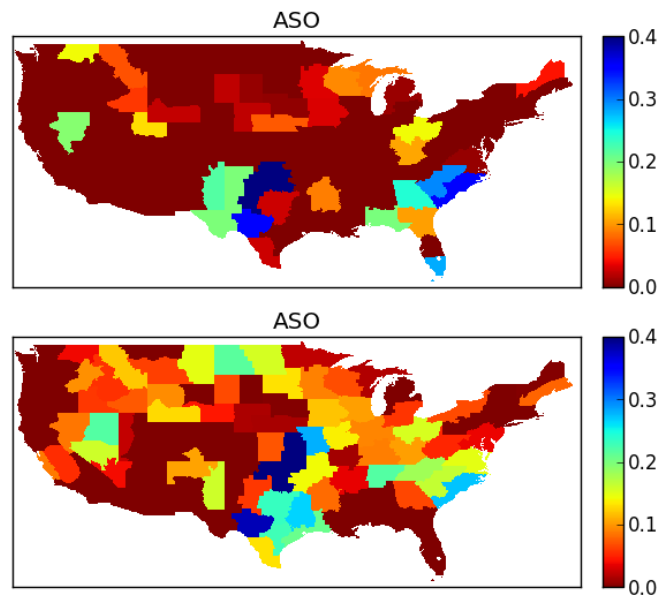


Figure 9: The differences in the ASO forecasts when using the combined model and just the prior month's NINO3.4 (top subplot) versus the prior three month's NINO3.4 (bottom subplot).

APPENDIX B:

Paper was published in Geophysical Research Letters, 2011.

**Decadal Prediction of Colorado River Streamflow Anomalies Using Ocean-
Atmosphere Teleconnections**

Matthew B. Switanek¹, Peter A. Troch²

¹Hydrology and Water Resources, University of Arizona

1133 E James E. Rogers Way Rm. 320A,

Tucson, AZ 85721

²Hydrology and Water Resources, University of Arizona

1133 E James E. Rogers Way Rm. 320,

Tucson, AZ 85721

Abstract

The Atlantic Multidecadal Oscillation (AMO) and Pacific Decadal Oscillation (PDO) time series are used to forecast a decade ahead streamflow anomalies in the upper Colorado River at Lee's Ferry. In the instrumental record, we obtain unusually high decadal forecast skill that is statistically significant at the 95% confidence level, suggesting strong ocean-atmosphere-land teleconnection. In order to test whether such teleconnection existed in the past, we compare the retrospective forecast skill to the skills obtained using the available ocean-atmosphere teleconnection and streamflow reconstructions derived from tree rings. We find much lower skill in the reconstructed record. Using frequency analysis, we show that the streamflow and sea surface temperature oscillations in the instrumental records all have dominant low frequency periodicities (> 35 years) that explain much of the total variance. However, such dominant periodicities do not appear in the power spectra of the reconstructed records of AMO, PDO and streamflow. Given that these dominant low periodicities are likely responsible for the high prediction skill in the instrumental record, it remains uncertain whether reliable decadal streamflow predictions in the upper Colorado River basin will be possible in the years ahead.

1. Introduction

Despite recent progress in seasonal to annual hydroclimate predictions based on ocean-atmosphere teleconnections induced by phenomena such as ENSO and PDO

[*Bracken et al.*, 2010; *Sankarasubramanian et al.*, 2008; *Switanek et al.*, 2009], little is known about how such teleconnections affect weather and water availability at longer time scales. Long-term anomalies in water availability, such as multi-year droughts, can significantly affect societal and environmental health. Given the natural variability of climate, regions that have faced droughts in the past will undoubtedly experience future events of similar magnitude and duration [*Cook et al.*, 2004; *Meko et al.*, 2007]. Being able to forecast the magnitude and timing of decadal-length droughts allows for better water management and subsequently improved municipal and agricultural planning.

Sea surface temperature (SST) anomalies in both the Atlantic and the Pacific oceans have been proposed as drivers of low frequency ocean-atmosphere-land teleconnections that could modulate or influence regional hydro-climates [*Barlow et al.*, 2001; *Ellis et al.*, 2010; *McCabe and Palecki*, 2006; *Nigam et al.*, 1999; *Nigam et al.*, 2011; *Tootle and Piechota*, 2006]. The AMO (Atlantic Multidecadal Oscillation) is defined as the average SST over the north Atlantic (between the equator and 70N; *Guan and Nigam*, 2009), while the PDO (Pacific Decadal Oscillation) is defined as the leading principal component of SSTs in the Pacific northward of 20N. *Hidalgo* [2004] and *McCabe et al.* [2007] have shown that there have been below/above average decadal flows in the Upper Colorado River basin at Lee's Ferry (river flow gauging station near Lake Powell that receives runoff from the Upper Colorado) when AMO is positive/negative and PDO is negative/positive. Therefore, in this study we address the following question: can the AMO and PDO time series, as expressions of ocean-climate

processes and their associated teleconnections, be used to provide statistically significant skillful decadal forecasts of hydro-climate in the upper Colorado River basin?

This study first develops a statistical method that uses prior decadal averages of AMO and PDO to forecast next decade streamflow anomalies. Additionally, we test these forecasts for statistical significance. Second, we use tree ring reconstructions of streamflow, AMO and PDO to see whether there is forecasting skill in the period preceding the instrumental record. We then compare the forecast skills of the instrumental and reconstructed records.

2. Data and Analysis

Observed naturalized flows for the Colorado River, at Lee's Ferry, were produced by the Bureau of Reclamation [*Prairie et al.*, 2005], while the tree-ring reconstruction of streamflow at the same location was performed by *Meko et al.* [2007] (all data used are provided as supplemental material). The observed naturalized flows currently exist for the years 1906-2007, while the reconstructions range between 762-2005. Additionally, the observed time series of the AMO [*Enfield et al.*, 2001] and PDO [*Mantua et al.*, 1997] indices can be obtained from NOAA at <http://www.esrl.noaa.gov/psd/data/climateindices>. The AMO and PDO have observed records that cover the years 1856-2009 and 1900-2009, respectively. Reconstructions of AMO and PDO were obtained from NOAA's Paleoclimatology website <http://www.ncdc.noaa.gov/paleo/recons.html>. The reconstruction of AMO [*Gray et al.*,

2004] is for the time period 1567-1990, while the reconstructions of PDO [D'Arrigo *et al.*, 2001; Biondi *et al.*, 2001; MacDonald and Case, 2005; Shen *et al.*, 2006] are for the time periods 1700-1979, 1661-1991, 993-1996 and 1470-1998, respectively.

The observed and reconstructed streamflow and AMO/PDO data are subjected to smoothing using a ten-year running mean (from now on referred to as 10yrRM) [Hurkmans *et al.*, 2009; Mauget, 2004; O'Lenic *et al.*, 2007]. The resulting time series are expressed as values corresponding to the last year of the 10yrRM. For example, the last 10yrRM value is 2007 and corresponds to the years 1998-2007.

We first tested the hypothesis that the previous decades' observed 10yrRM AMO and PDO values could be used to make relevant and statistically significant predictions of next decade streamflow anomalies at Lee's Ferry. In this effort, retrospective forecasts were made for the last forty 10yrRMs (1968-2007). Plot A of Figure 1 shows 10yrRMs of AMO and PDO with the 10yrRMs of Lee's Ferry streamflow lagged by 10 years. The 10yrRMs of AMO and PDO have a correlation coefficient of .02, and are therefore treated as independent time series. The 10yrRMs are expressed as z-scores, or standard deviations from the mean. The + and x symbols correspond to above and below average streamflow, respectively, while the magnitudes of the departures are reflected by the size of the symbols. For reference we provide the size of the symbols when 1- σ and 2- σ variability would occur.

Using smoothed 10yrRMs of streamflow requires that we consider how the forecasts might be influenced by autocorrelation. However, it is only the lag-10

autocorrelation (e.g., pairing a streamflow value corresponding to the decade 1971-1980 with a value from 1981-1990) that necessitates attention. This is because even though our window moves a single year and, subsequently, overlap exists in the forecasts, there is not any overlap between the information used to derive the forecast and the forecasted value itself.

Even though no streamflow data from the time we are forecasting is used, there still could be persistence that could affect the decadal forecasts. To observe if this persistence affects the independence of the smoothed data from one distinct decade to the next, we forecast decadal values of streamflow using the last decadal streamflow value and the lag-10 autocorrelation. We find that making forecasts using persistence in conjunction with the climatology would give skill that is worse than using the climatology alone. Therefore, we assume that the forecasted decadal streamflow is independent of the prior decade's value, and we compare our forecast skills to the climatology alone. This is explained in more detail in the Results section.

Plot B of Figure 1 is used to illustrate our methodology. Plot B shows the values of AMO and PDO from the year 1915 (referring again to the years 1906-1915) through the year 1968, paired with Lee's Ferry streamflow values that are between 1925 and 1978. We use the statistical relationships from this time period to retrospectively forecast Lee's Ferry streamflow for the years 1979-1988, using SST information only up through 1978. The forecasts are made as standard deviations from the mean (using the data that was available prior to the forecast). The black circle in plot B shows the AMO/PDO

value for 1969-1978. A Euclidean distance measure (the spatial distance between the points in the scatter plot) is used to make all of the forecasts of decadal streamflow. We obtained the best retrospective forecast skill by averaging the streamflow from the closest seven points with respect to the most recent AMO/PDO value. The closest points, in the current example, are shown within the gray circle in plot B of Figure 1. The skill measure used is defined as $skill=1-[\Sigma(X_{obs}-X_{sim})^2/\Sigma(X_{obs}-X_{clm})^2]$, where X_{obs} and X_{sim} are the time series of the observations and simulations (or forecasts), respectively, and X_{clm} is the climatological mean of all the available prior streamflows. Forecasts that perform worse, equal to, or better than the climatology have skill scores that are less than zero, zero, or greater than zero, respectively.

In addition to testing for statistically significant decadal forecast skill of streamflow at Lee's Ferry using the observed record, it is desirable to see if the skill in the reconstructed record is of similar magnitude. Reconstructions of AMO and PDO are therefore used to forecast decadal Lee's Ferry reconstructed values. The reconstructions were subdivided into moving windows of ninety-three 10yrRMs (which is the length of the observed record). Then, similarly to the observed record, the last 40 values of each reconstructed window at Lee's Ferry were retrospectively forecasted using the closest points from a Euclidian distance measure. For example, the last 40 decadal values of the reconstructed Lee's Ferry are forecasted from the time period 1608-1700. This skill value corresponding to the forecasts of the decadal values for 1661-1700 is attributed to the year 1700. The same procedure is then performed using the years 1609-1701 to obtain

another skill value for that subset of the reconstructions. With this approach, a time series of skills can be obtained to compare with the skill value of the observed record.

3. Results

The forecasts of decadal streamflow at Lee's Ferry, for the instrumental record, are shown in contrast to the observations in Figure 2. The skill of decadal prediction of Lee's Ferry streamflow is 0.44 and is statistically significant against the climatology at the 97% confidence level. Statistical significance of the skill against the climatology is calculated using a Monte Carlo approach. Random values are smoothed in the same manner as the climate indices and streamflow data. This is done by first selecting 49 random values from a gamma distribution that is fit to the observed annual streamflow data. The values are then smoothed with a 10-value moving window. Next, this smoothed vector has the mean subtracted out and divided by the standard deviation of the observed 10yrRM streamflow data. This randomly generated set of predictions is then used to obtain a corresponding skill. This process is replicated 10,000 times with a skill measure calculated each time. Skill values of .37 and .23 correspond to 95% and 90% statistical significance levels, respectively. Additionally, we found the skill associated with making predictions using both past climatology and persistence of the decadal streamflow data. This was done by first acquiring the lag-10 autocorrelation of the smoothed data preceding the forecast time. Since we are dealing with z-scores of decadal streamflow, the correlation coefficient is the same as the slope of the regression line. A forecast is

then made for the next decade by multiplying the z-score of the most recent completed decade by the lag-10 autocorrelation value. Using persistence to make forecasts for the last forty 10yrRMs leads to a skill of -.07. This means that persistence with climatology provides worse forecasts than the climatology alone. Therefore, we are confident in the statistical significance levels obtained with the Monte Carlo approach explained above.

Each of the four PDO reconstructions were used together with the sole AMO reconstruction to retrospectively forecast decadal streamflows at Lee's Ferry. The different combinations of reconstructions and their associated skill through time can be seen in Figure 3. It can be seen that the skill obtained in the instrumental record (0.44, shown as the bold gray dashed line) is rarely met or exceeded with any of the combinations of reconstructions over their respective time periods. The set of reconstructed skills matches or exceeds the instrumental record about one percent of the time, and the time-averaged skills using the reconstructions were -.28, -.26, -.35 and -.33 (green, red, blue and black, respectively in Figure 3). It is interesting to note that correlations obtained between concurrent decades do not necessarily translate into skillful forecasts. We observe the largest correlation coefficient for concurrent decades is .62 (using reconstructions of PDO [*Biondi et al.*, 2001] and Lee's ferry streamflow), while it is -.18 when streamflow is lagged by 10 years.

4. Discussion and Conclusions

This study first used the instrumental records to show that there is statistically

significant skill in forecasting the next decade of Lee's Ferry streamflow using the previous decadal values of AMO and PDO. This by itself is a remarkable result given the strength of the forecast skill (0.44 at 97% significance level). However, with all available combinations of reconstructed teleconnections, the level of decadal forecast skill of streamflow at Lee's Ferry is drastically less than what is seen in the instrumental record. What could explain this dramatic shift in decadal forecast skill? Figure 4 provides frequency analyses of the instrumental and reconstructed records of AMO, PDO and Lee's Ferry streamflow. The fact that all three time series have a dominant low frequency in the instrumental records can explain why we observe such a high level of forecast skill. All three of the observed time series have dominant periodicities greater than 35 years. Forecasting proves to be quite skillful when all three variables have much of their variance explained by similar low frequency oscillations. However, we do not see such dominant periodicities in the power spectra of the reconstructed records of AMO, PDO and streamflow. Is there an underlying physical mechanism that has caused these variables to align in the instrumental record, or has this happened by chance?

There exists the possibility that there is a physical relationship between the sea surface temperature oscillations (characterized by AMO/PDO) and Colorado streamflow through ocean-atmosphere-land teleconnections, as suggested by several studies [*Barlow et al.*, 2001; *Hidalgo*, 2004; *Nigam et al.*, 2011; *Tootle and Piechota*, 2006]. If this is the case, we would expect that the dominant periodicities will continue to be aligned for the three variables, and the skill in forecasting decadal streamflow will persist. Using the

reconstructions, however, we do not see alignment in the periodicities of these three variables. This is reflected in the poor forecast skills in the reconstructions. There is a more obvious physical relationship, though, between tree ring growth and the amount of water that has fallen in a basin and ending up as streamflow, than between SSTs and regional hydro-climate (e.g., an El Niño year does not always provide a spatial rainfall pattern like we expect). Given this scenario, we can compare the distributions and periodicities of the instrumental records of AMO and PDO with the Lee's Ferry reconstruction. We observe that the dominant periodicities of AMO and PDO (between 50 and 70 years) are not dominant periodicities in the Lee's Ferry reconstruction.

These results and analyses raise several questions. It remains unclear whether the low frequency variability of climate indices, such as AMO and PDO, are accurately preserved in the tree-ring reconstructions of the different time series. If this is not the case it could explain the loss of decadal forecasting skill in the paleo record. Also, is there a dynamic connection between SSTs (that comprise the AMO/PDO) and precipitation in the regions where tree rings were used, or are the AMO/PDO reconstructions strictly statistical? This is a question concerning causality. ENSO is, at some level, dynamically understood and the most well known of the SST climate teleconnections. However, we still cannot quantify precipitation in regions affected by ENSO with good accuracy. Therefore, even if strong correlations exist between tree rings and the instrumental records of AMO/PDO, these are statistical relationships that are not necessarily indicative of our understanding of any physical mechanisms involved. Due to this fact and the

general uncertainty associated with the reconstructed teleconnections, caution should be exercised when interpreting the results derived using these time series.

Enfield and Cid-Serrano [2006] and *Gangopadhyay and McCabe* [2010] have presented probabilistic methods to project teleconnections or streamflow given the time since the last regime shift. Methods such as these could be used to supplement our decadal streamflow forecasts derived from the AMO and PDO indices. However, these methods would only extend upon the statistical nature of our forecasts. More research is required to define physical links between the SSTs that make up the AMO/PDO and streamflow [*Cook et al.*, 2007; *Seager et al.*, 2005]. When using the methodology herein to forecast future decadal streamflows, two results require consideration: 1) There is a large gap between the forecasting skill in the instrumental and reconstructed records; and 2) The dominant periodicities seen in the instrumental AMO/PDO are not present in the Lee's Ferry streamflow reconstructions. These results appear to foretell a future of less skillful forecasts of Lee's Ferry decadal streamflow than the instrumental record indicates. Time will reveal whether the hydrologic regime in the upper Colorado River basin will continue to shift in phase with AMO and PDO time series.

Aknowledgments

The authors would like to thank Terry Fulp, Jim Prairie and the entire Bureau of Reclamation, Lower Colorado Regional Office, for funding this study. Also, the editors and reviewers at GRL provided invaluable suggestions that assisted us in shaping the

current version of the manuscript.

References

- Barlow, M., S. Nigam, and E. H. Berbery (2001), ENSO, Pacific decadal variability, U.S. summertime precipitation, drought, and stream flow, *J. Climate*, *14*, 2105-2128.
- Bracken, C., B. Rajagopalan, and J. Prairie (2010), A multisite seasonal ensemble streamflow forecasting technique, *Water Resour. Res.*, *46*, W03532, doi:10.1029/2009WR007965.
- Biondi, F., A. Gershunov, and D. R. Cayan (2001), North Pacific decadal climate variability since 1661, *J. Climate*, *14*, 5-10.
- Cook, E. R., C. A. Woodhouse, C. M. Eakin, D. M. Meko, and D. W. Stahle (2004), Long-Term aridity changes in the western United States, *Science*, *306*, 1015-1018.
- Cook, E. R., R. Seager, M. A. Cane, and D. W. Stahle (2007), North American drought: reconstructions, causes, and consequences, *Earth Sci. Rev.*, *81*, 93-134.
- D'Arrigo, R., R. Villalba, and G. Wiles (2001), Tree-ring estimates of Pacific decadal climate variability, *Climate Dynam.*, *18*(3-4), 219-224.
- Ellis, A. W., G. B. Goodrich, and G. M. Garfin (2010), A hydroclimatic index for examining patterns of drought in the Colorado River Basin, *Int. J. Climatol.*, *30*, 236-255, doi:10.1002/joc.1882.
- Enfield, D. B., A. M. Mestas-Nunez, and P. J. Trimble (2001), The Atlantic multidecadal oscillation and its relationship to rainfall and river flows in the continental U.S.,

Geophys. Res. Lett., 28, 2077-2080.

Enfield, D. B., and L. Cid-Serrano (2006), Projecting the risk of future climate shifts, *Int. J. Climatol.*, 26, 885-895, doi:10.1002/joc.1293.

Gangopadhyay, S., and G. J. McCabe (2010), Predicting regime shifts in flow of the Colorado River, *Geophys. Res. Lett.*, 37, L20706, doi:10.1029/2010GL044513.

Gray, S. T., L. J. Graumlich, J. L. Betancourt, and G. T. Pederson (2004), A tree-ring based reconstruction of the Atlantic multidecadal oscillation since 1567 A.D., *Geophys. Res. Lett.*, 31, L12205, doi:10.1029/2004GL019932.

Guan, B., and S. Nigam (2009), Analysis of Atlantic SST variability factoring interbasin links and the secular trend: clarified structure of the Atlantic multidecadal oscillation, *J. Climate*, 22, 4228-4240.

Hidalgo, H. G. (2004), Climate precursors of multidecadal drought variability in the western United States, *Water Resour. Res.*, 40, W12504, doi:10.1029/2004WR003350.

Hurkmans, R., P. A. Troch, R. Uijlenhoet, P. Torfs and M. Durcik (2009), Effects of climate variability on water storage in the Colorado River basin, *J. Hydrometeorol.*, 10, 1257-1270.

MacDonald, G. M., and R. A. Case (2005), Variations in the Pacific decadal oscillation over the past millennium, *Geophys. Res. Lett.*, 32, L08703, doi:10.1029/2005GL022478.

Mantua, N. J., S. R. Hare, Y. Zhang, J. M. Wallace, and R. C. Francis (1997), A Pacific

- interdecadal climate oscillation with impacts on salmon production, *B. Am. Meteorol. Soc.*, 78, 1069-1079.
- Mauget, S. A. (2004), Low frequency streamflow regimes over the central United States: 1939-1998, *Climate Change*, 63, 121-144.
- McCabe, G. J., and M. A. Palecki (2006), Multidecadal climate variability of global lands and oceans, *Int. J. Climatol.*, 26, 849-865, doi:10.1002/joc.1289.
- McCabe, G. J., J. L. Betancourt, and H. G. Hidalgo (2007), Associations of decadal to multidecadal sea-surface temperature variability with upper Colorado River flow, *J. Am. Water Resour. As.*, 43(1), 183-192, doi:10.1111/j.1752-1688.2007.00015.x.
- Meko, D. M., C. A. Woodhouse, C. A. Baisan, T. Knight, J. J. Lukas, M. K. Hughes, and M. W. Salzer (2007), Medieval drought in the upper Colorado river basin, *Geophys. Res. Lett.*, 34, L10705, doi:10.1029/2007GL029988.
- Nigam, S., M. Barlow, and E. H. Berbery (1999), Analysis links Pacific decadal variability to drought and streamflow in the United States, *EOS, Transactions, AGU.*, 80, 621,622,625.
- Nigam, S., B. Guan, and A. Ruiz-Barradas (2011), Key role of the Atlantic multidecadal oscillation in 20th century drought and wet periods over the Great Plains, *Geophys. Res. Lett.*, 38, L16713, doi:10.1029/2011GL048650.
- O'Lenic, E. A., D. A. Unger, M. S. Halpert, and K. S. Pelman (2007), Developments in operational long-range climate prediction at CPC, *Weather Forecast*, 23, 496-515.
- Prairie, J., and R. Callejo (2005), Natural flow and salt computation methods, U.S. Dep.

- of Interior, Salt Lake City, Utah, (Available at <http://www.usbr.gov/lc/region/g4000/NaturalFlow/NaturalFlowAndSaltComptMethodsNov05.pdf>).
- Sankarasubramanian, A, U, Lall, and S. Espinueva (2008), Role of retrospective forecasts of GCMs forced with persisted SST anomalies in operational streamflow forecasts development, *J. Hydrometeorol.*, *9*, 212-227.
- Seager R., Y. Kushnir, C. Herweijer, N. Naik, and J. Velez (2005), Modeling of tropical forcing of persistent droughts and pluvials over western north America: 1856-2000, *J. Climate*, *18*, 4065-4088.
- Shen, C., W. C. Wang, W. Gong, and Z. Hao (2006), A Pacific decadal oscillation record since 1470 AD reconstructed from proxy data of summer rainfall over eastern China, *Geophys. Res. Lett.*, *33*, L03702, doi:10.1029/2005GL024804.
- Switanek, M. B., P. A. Troch, and C. L. Castro (2009), Improving seasonal predictions of climate variability and water availability at the catchment scale, *J. Hydrometeorol.*, *10*, 1521-1533.
- Tootle, G. A., and T. C. Piechota (2006), Relationships between Pacific and Atlantic ocean sea surface temperatures and U.S. streamflow variability, *Water Resour. Res.*, *42*, W07411, doi:10.1029/2005WR004184.

Figures

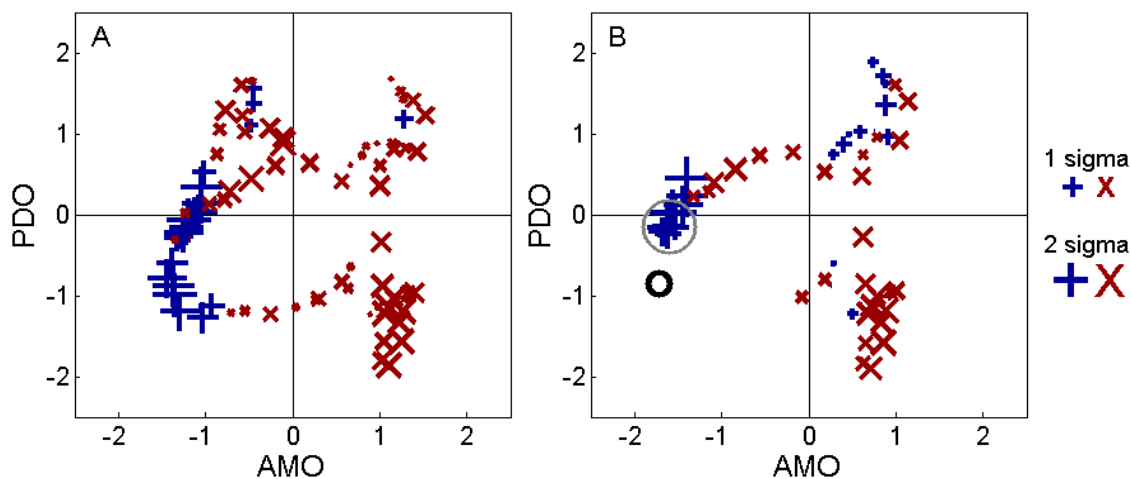


Figure 1: Plot A shows standardized departures of Lee's Ferry streamflow lagged 10 years behind departures of AMO and PDO. All values are 10-year running means. The AMO and PDO values are the 10yrRMs between 1915-1997, while the streamflows at Lee's Ferry are between 1925-2007. The + and x symbols correspond to above and below average streamflow, respectively, while the magnitudes of the departures are reflected by the size of the symbols. Plot B shows the initial 54 values (10yrRMs between 1915-1968) of AMO and PDO with Lee's Ferry streamflows lagged by 10 years. The black circle shows an example of the average AMO/PDO over the previous ten years (1978 10yrRM) that is used to predict streamflow for the following decade (1988 10yrRM). The gray circle surrounds the values that are used to make the forecast.

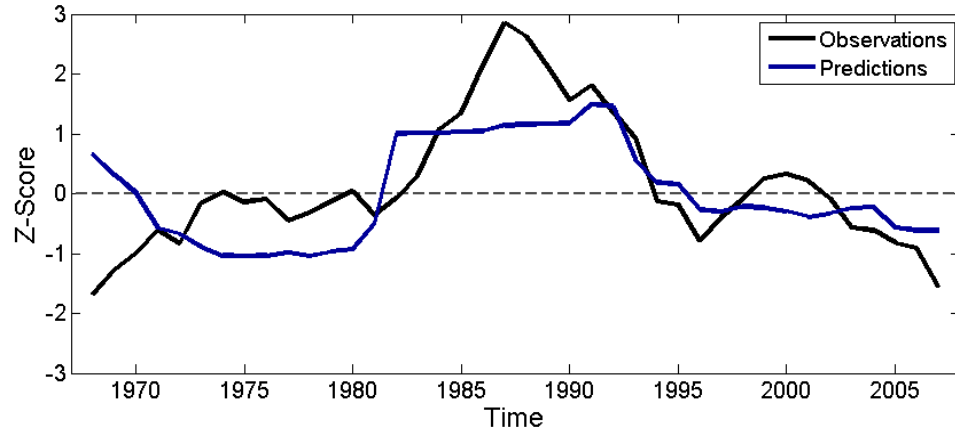


Figure 2: Observations and predictions of Lee's Ferry streamflow. The x-axis corresponds to the last year of the 10-year period of interest.

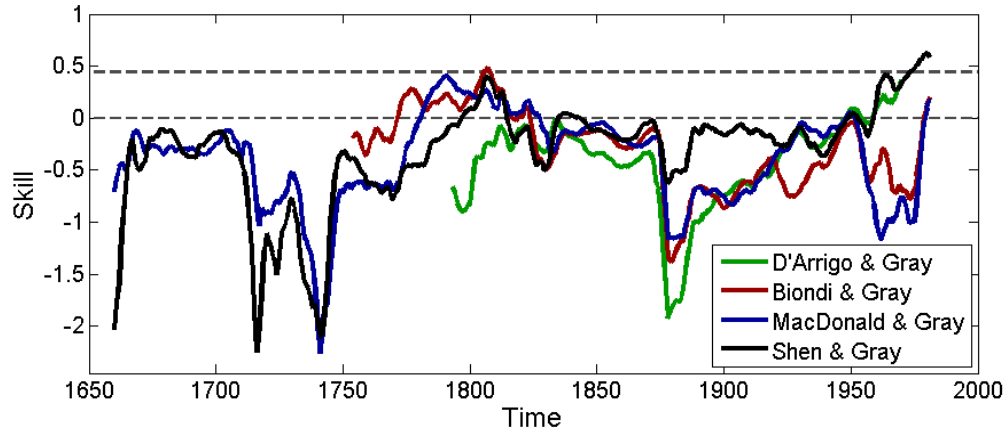


Figure 3: The change in predictive skill through time when using the different combinations of reconstructions. Each skill value is obtained using the last forty 10yrRMs from a discrete time period equal in length to the observed time series. The thinner gray line (Skill=0) provides a reference skill equal to the climatology. The thicker gray dashed line (Skill=.45) shows the skill from the instrumental record.

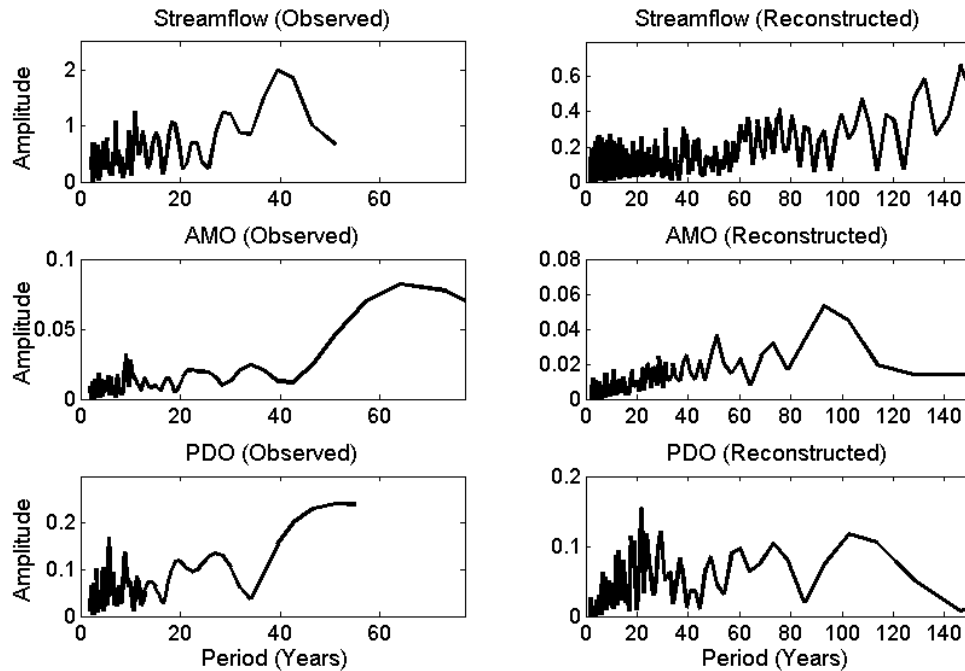


Figure 4: Frequency analyses of the observed and reconstructed records of streamflow at Lee's Ferry, AMO and PDO (reconstruction of PDO is *Biondi et al., 2001*). The x-axes are the periods, while the y-axes are the amplitudes explained by each period. The left column all extend 77 years along the x-axis, which is half of the length of the AMO time series (statistically relevant periodicities require two cycles). There are clear dominant periods in the observed records that are seen at longer than 35 years. The reconstructed records, down the right column, do not have comparable dominant frequencies.

APPENDIX C:

Paper was prepared to be submitted to a journal.

**Dynamically Downscaled and Bias-Corrected Climate Projections Exhibit a Drier
Future for Southwest River Basins**

Matthew B. Switanek, Peter A. Troch, Matej Durcik and Eleonora Demaria

Department of Hydrology and Water Resources, University of Arizona, Tucson, Arizona

Christopher L. Castro, Hsin-I Chang, and Thang Luong

Department of Atmospheric Sciences, University of Arizona, Tucson, Arizona

ABSTRACT

Due to limited water availability, climate change can have particularly dramatic effects in the semi-arid Southwestern United States. Global general circulation models (GCMs) have shown climate change is expected to further stress the water resources of this region. GCMs currently are too coarse to resolve regional scale physical processes. Regional climate models (RCMs) such as the Weather and Research Forecasting (WRF) dynamically downscale GCMs to provide more realistic realizations at higher resolutions. The HadCM3 and MPI- ECHAM5 GCMs were used to force the WRF model. The resulting climate was then bias corrected and used to force the Variable Infiltration Capacity model through the year 2080 for the Salt and Verde basins and the Rio Grande headwaters. For the HadCM3 model, we project a 23%, 22% and 20% decrease in average future streamflow (in reference to the past) for the Salt, Verde and Rio Grande, respectively. While the MPI model is projecting decreases of 43%, 38% and 31%, respectively.

1. Introduction

Climate change in the 21st century is expected to substantially impact regional water supplies across the world. The population and agricultural centers in the southwestern United States are particularly susceptible to changes in streamflow quantity. This is due to this region's lack of abundant surface water reserves and a dwindling supply of groundwater. The Colorado River Basin and the headwaters of the Rio Grande

River are the lifelines of the Southwest region. These rivers are heavily regulated and, as a result, any reductions in these streamflows would severely impact the region's economic and environmental health. Therefore, it is essential to understand how climate change could affect future water resources in river basins such as the Colorado and Rio Grande.

The General Circulation Models (GCMs) used in the IPCC (Intergovernmental Panel on Climate Change), on average, project that global mean surface temperatures are going to rise (Barnett et al. 2005; Christensen et al. 2004; Held and Soden 2006; Kharin and Zwiers 2000, 2005). More specifically to the Southwest region, the GCMs have a consensus on the direction of temperature trends (increasing), while precipitation is expected to decrease at the mid-latitudes (Dominguez et al. 2012). GCMs are invaluable in providing general forecasts of future climate, though they are too coarse (typically 150-300 km) to provide the detail that is necessary to accurately assess regional dynamics (Castro et al., 2005; Maurer and Hidalgo, 2008; Woods et al., 2004; Von Storch et al., 1993). Ideally, in an effort to understand the role that climate change plays in a particular region such as the Southwest, one would downscale GCM forecasts with a Regional Climate Model (RCM) that produce variables that preserve a level of spatial coherence and physical plausibility. This physical plausibility of the RCMs allows for non-stationarity in future realizations of the climate variables (Milly, 2008). Until recently, dynamically downscaling multi-decade simulations of General Circulation Models (GCMs) were not reasonable for environmental impact studies of relatively large regions

(Maurer et al., 2008; Sungwook et al., 2012). This was due to the amount of time and resources required to run an RCM for many decades. Past climate change studies have typically statistically downscaled GCMs. Statistical downscaling is efficient and provides an important glimpse into potential environmental impacts the future contains. Importantly, however, statistical downscaling cannot account for non-stationarity. While the methodology can incorporate trends to the data, any extreme events or systematic changes to a climate variable's mean and variance cannot be reasonably implemented (Dominguez et al., 2012). Additionally, any nonlinearities inherent to the physical system might not be correctly applied to climate variables relying on statistics alone.

These changes to the climate subsequently lead to earlier timing of snowmelt (Barnett et al., 2005; Cayan, 2000; Stewart et al., 2004). Additional studies have pointed out that the streamflow distributions may not only be shifting, but also may be decreasing/increasing in volume as well (Christensen et al., 2004; Allen et al., 2002; Acharya et al., 2012). Goa et al. (2011) used RCMs to dynamically downscale three GCMs and found two projected a 16% decrease in streamflow in the Colorado River basin, while one projected a 5% increase. These values were calculated as relative changes between the periods 2040-2069 and 1970-1999 using the raw, modeled climate data. Our study also uses an RCM to dynamically downscale two GCMs, but we bias correct the RCM climate variables before forcing the hydrologic model. Additionally, we look at relative changes over a longer period of projected time (~70 years). Finally, we investigate the hydrologic response at selected subbasins in the Colorado river and also

add the headwaters of the Rio Grande river.

Allen and Ingram (2002) write, "In the absence of objective probabilistic forecasts with numerical models that systematically investigate the range of possible responses of the hydrologic cycle to anthropogenic climate change, we have here attempted to constrain the expected changes by other means." Ideally, one would like to dynamically downscale many of the GCMs used in the IPCC report under a range of different climate scenarios. With the continued expansion of computational resources, this will soon be possible. Before dynamically downscaling multiple decades of GCMs becomes the new norm, the authors attempt to provide an first glimpse into the climatic and hydrologic changes that are part of the distribution of future realizations. We have chosen two GCMs that have historically performed well in simulating the climate over the southwestern United States. This study used two dynamically downscaled GCMs for the region encompassing the southwestern United States and northwestern Mexico. The two GCM climate models used were the HadCM3 and the MPI-ECHAM5. They were downscaled with the Weather and Research Forecasting (WRF) regional scale climate model. This study sets out to investigate whether the overall quantity of streamflow is projected to change in selected subbasins of the Colorado and Rio Grande rivers.

2. Data and Methodology

a. Study Locations and Data

The Salt and Verde basins and Rio Grande headwaters are shown in Figure 1.

USGS streamflow gauges 09498500, 09508500, and 08220000 are used as the hydrologic outflow points for the Salt, Verde, and Rio Grande, respectively. The Salt and Verde basins have areas of 11,100 km² and 15,200 km² above the streamflow gauges, while the Rio Grande headwaters has an area of 3,400 km². Average streamflows of 2.09*10⁶ m³/day, 2.03*10⁶ m³/day, and 1.43*10⁶ m³/day are seen at the Salt, Verde and Rio Grande gauges, respectively.

The Weather and Research Forecasting (WRF) model has been used extensively as a regional-scale atmospheric model. Data from two General Circulation Models (GCMs) from IPCC Fourth Assessment Report, that have historically performed well over the Southwest, were chosen to force the WRF model. These models are the HadCM3 and the MPI-ECHAM5 (MPI from here on). WRF dynamically downscales climate data from these two GCMs under the A1B (medium emission scenario or 'Business as Usual', CO2 concentration 700ppm by 2100) scenario at a resolution of 32 km. Additionally, an atmospheric reanalysis data set (NCEP-NCAR) was used to provide a measure of how well the WRF model can simulate regional-scale weather events that comprise the climate. Later in the paper, any time we refer to the HadCM3, MPI, and NCAR, we are more specifically referring to the dynamically-downscaled climate data from these GCMs.

The hydrologic modeling is performed using the Variable Infiltration Capacity (VIC) model. The VIC model represents surface and subsurface hydrologic processes on spatially distributed grid cells. Distinguishing characteristics of the model include the

representation of subgrid scale variability in vegetation coverage, topography, precipitation, and soil moisture storage capacity. The subsurface is represented by three soil layers. Evapotranspiration can occur from soil moisture in the three layers, while slow response runoff or baseflow is only generated from the third layer. To represent the sub-grid spatial variability in soil moisture storage, the model assumes that the infiltration capacity is a non-linear function of the soil moisture storage within the gridcell. Simulations in this study were performed at a daily time step with a 12.5 km resolution (1/8 degree).

b. Model Calibration and Bias Correction

1) VIC MODEL CALIBRATION

Calibration of the VIC model was performed using Ed Maurer's climate data set as observed data (Maurer et al., 2002). VIC was calibrated on daily streamflow values using the Shuffled Complex Evolution algorithm. The Kling-Gupta efficiency (KGE) parameter (Gupta et al., 2009) was used as the objective measure of skill between modeled and observed streamflows. The KGE is defined as

$$KGE = 1 - \sqrt{(1-a)^2 + (1-b)^2 + (1-r)^2}, \quad (1)$$

where a is the ratio of the means, b is the ratio of the coefficient of variations, and r is the correlation coefficient. The KGE skill measure provides the optimum parameter set that has the least Euclidian distance between simulations and observations. Typically, the measure will make sacrifices in correlation, with respect to another skill measure such as

the Nash-Sutcliffe efficiency parameter, but makes substantial improvements in bias and variance explained. During the calibration process, it became apparent that no amount of model calibration could reduce a substantial amount of positive bias (see Figure 2). The model was always predicting, on average, more streamflow. Given the methods of sampling streamflow versus precipitation, at the basin scale, we see streamflow data as being more certain than interpolated precipitation data. Therefore, in order to have the model perform better, we adjusted the precipitation data by a constant multiplier. This constant multiplier of precipitation was then an additional parameter in the model calibration. Figure 2 illustrates the effectiveness of the calibration procedure. The Salt and Rio Grande clearly show the amount of positive bias in the streamflow forecasts prior to calibration. Each component of the KGE was improved in the calibration process, except for the Rio Grande's correlation, which slightly decreased (a trade-off to drastically improve the bias and variance explained).

2) BIAS CORRECTION OF CLIMATE DATA

Bias correction of precipitation, temperature and wind were all performed independently. Bias corrections of precipitation, temperature and wind were all performed with a modified form of distribution mapping (Bárdossy and Pegram, 2011; Teutschbein and Seibert, 2012; Wood et al., 2004). We use a distributional mapping method with fitted gamma distributions for precipitation, and normal distributions for the other variables. The bias correction of precipitation had to meet a number of criteria.

First, the distributions of the simulated and observed precipitation had to closely match for each subset time of the year. Second, the frequency of rain events had to match. Third, changes in the distributions and frequencies of precipitation events, at different seasons, had to be preserved.

To begin with, precipitation data was bias corrected on a 21-day moving window (precipitation, maximum temperature, minimum temperature, and wind all use a 21-day moving window to compute the bias corrected data for a particular day). Consider the bias correction of the precipitation values of HadCM3 and MPI data for all years that overlap with observations (1968-2010 and 1950-2010, respectively) for the date January 11. Positive precipitation values between January 1st and January 21st for these years were used to fit the gamma distribution parameters a and b for the observed and simulated data. For each value of precipitation (x -axis on the fitted gamma cumulative distribution function (CDF)) that occurred on January 11th, its corresponding cumulative distribution is found (y -axis on the same CDF). The same cumulative distribution is then located on the fitted gamma distribution of the observations for the same day. And finally, the bias corrected precipitation would be the corresponding value on the x -axis. Next, we need to account for the difference between the amount of rain days for the observations and the projected climate. The climate models were always forecasting more rain days. Therefore, we randomly removed precipitation events to match the percentage of rain days, seen in the observed period, for each 21-day moving window.

The next step was to bias correct the future time period of precipitation. First, the

percentage differences between the mean and standard deviations were used to shift the observed gamma distribution. With a two parameter gamma distribution, the mean and the variance are defined as $\alpha*\beta$ and $\alpha*\beta^2$, respectively. Therefore, it is clear that for a gamma distribution $\beta = \text{variance}/\text{mean}$ and $\alpha = \text{mean}/\beta$. We find the mean and the variance of both the gamma distributions in the time overlapping the observations (overlapping time period referred to as OLTP, 1968-2010 for HadCM3 and 1950-2010 for MPI) and the projected time periods (projected time period referred to as PJTP, 2011-2079 for HadCM3 and 2011-2080 for MPI). The ratio by which the mean and the variance of the PJTP differs with respect to the OLTP is then multiplied by the mean and variances of the observed distribution. We then can use these new mean and variance values to solve for the α and β of a new gamma distribution. This gamma distribution will then have the same proportional shift, with reference to the observational distribution, as the shift between projected and past precipitation. The first two steps of the bias correction, outlined in this paragraph, are then repeated using the shifted observed gamma distribution to bias correct future precipitation values.

The well established bias-correction and spatial downscaling (BCSD) methodology (Wood et al., 2004) is different than what is presented here in the following ways. Empirical distributions are used for BCSD, while we map to any location on a fitted gamma distribution. BCSD matches the month, then samples from one of the years. Second, we match the closest whole number of days of rain about our moving window. If one starts with a model with more rain days, this appears to be preserved in BCSD,

though each value is scaled so that the monthly means match up. Because streamflow can respond differently to the same precipitation amount spread over a varied number of days, we attempt to preserve the observed frequency of rain events. Lastly, we allow both the scale and shape parameters of the distribution in the PJTP to change. Therefore, any increase in the mean or the variance projected in the model with respect to the OLTP is proportionally preserved. The BCSD method, however, will increase or decrease the projected mean monthly values if the ratio of variance to mean is not precisely the same for both the OLTP and observations. As a result of these reasons, we believe that these small, but important, differences make our bias correction a better choice when dealing with projected future climate.

The bias correction of maximum and minimum temperature were also performed using a 21-day moving window. In bias correcting the temperatures, the means and variances of the OLTP for the HadCM3 and MPI models are shifted to match those of observations. However, the trends seen in the models are preserved. This is so that the models' physical representations of a potential future climate is not constrained by the trends that we have observed in the past. Future trends can be different than what the past suggests. Lastly, and similarly to precipitation, differences in the distributions and the trends between the OLTP and the PJTP were preserved.

Often a trend was seen in both the observed and simulated temperatures (e.g., moving through the years for a specific day). This trending inflates the variance. This is due to the fact that the differences between the values in a time series and a fixed mean is

greater than the differences between the values and their accompanying trend line (provided that there is a non-zero trend). Therefore, the standard deviation of temperature for a particular day's window is

$$T_{std} = \sqrt{\sum((T - T_{reg})^2) / (n-1)} \quad (2)$$

where T is the temperature time series for a specific day, T_{reg} is the regression line of the temperature time series, and n is the number of values in T . The bias correction of maximum and minimum temperature values in the OLTP was calculated as

$$T_{bc} = T_{mod} + T_{trnd_mov} - T_{trnd_ind} \quad (3)$$

where T_{bc} is bias corrected temperature and

$$T_{mod} = T_{obs_mean} + (T_{gcm} - T_{gcm_mean}) * (T_{obs_std} / T_{gcm_std}) \quad (4)$$

and

$$T_{trnd_mov} = T_{gcm_trnd_mov} + (T_{obs_mean} - T_{gcm_mean}) \quad (5)$$

and T_{trnd_ind} is the regression line of T_{mod} . T_{bc} is the bias corrected maximum or minimum temperature. T_{mod} is the modified temperature data where T_{obs_mean} , T_{gcm_mean} , T_{obs_std} , and T_{gcm_std} are means and standard deviations of the observations and the OLTP GCM (HadCM3 or MPI) values within the moving window, respectively. T_{trnd_mov} is the adjusted 21-day moving window trend, where $T_{gcm_trnd_mov}$ is the moving window trend of the raw HadCM3 or MPI data. This provides a trend line of the OLTP GCM data with its mean identical that of T_{obs_mean} . Hence, the OLTP T_{bc} is found by first calculating the two time series of T_{mod} and T_{trnd_mov} . Second, the regression line of T_{mod} is obtained. Lastly, the bias corrected

temperature, T_{bc} , will be T_{mod} plus the moving window trend (T_{trnd_mov}) minus the time series of the individual day's trend (T_{trnd_ind}). Calculating T_{mod} does the work of the bias correction and shifts the mean and variance of the OLTP GCM temperatures to match those of observations. The act of adding T_{trnd_mov} and subtracting T_{trnd_ind} effectively is shifting the individual day's temperature trend to match that of the moving window trend.

Bias correcting temperature in the projected time period is very similar with a couple of small modifications. Equation 4 now becomes

$$T_{mod} = T_{obs_mean} + (T_{gcm2} - T_{gcm_mean2}) * (T_{obs_std}/T_{gcm_std2}) * (T_{gcm_std2}/T_{gcm_std1}) \quad (6)$$

where the subscripts 1 and 2 represent the overlapping and projected time periods, respectively. The additional term in equation 6, with respect to equation 4, increases or decreases the variance proportionally to the ratio of the standard deviations seen in the projected and overlapping time periods. Equation 6 reduces to

$$T_{mod} = T_{obs_mean} + (T_{gcm2} - T_{gcm_mean2}) * (T_{obs_std}/T_{gcm_std1}) \quad (7)$$

Lastly, equation 5 is now

$$T_{trnd_mov} = T_{gcm_trnd_mov2} + (T_{obs_mean1} - T_{gcm_mean1}) \quad (8)$$

where the trend line of the projected time period is further offset by the difference between the observed and OLTP temperatures.

Wind was bias corrected using 4 and 7, with wind in place of temperature, for the overlapping and projected time periods, respectively. The modified wind is the bias corrected wind because no statistically significant trending of wind was discernible, and therefore no trend adjustments were implemented.

3. Results

a) Calibration and Bias Correction

The results of the VIC model calibration are apparent in Figure 2. Prior to model calibration, the Salt, Verde and Rio Grande basins had KGE values of -.73, .17, and -.44, respectively (these values correspond to the subplots in the upper row of Figure 2). After model calibration, the Salt, Verde and Rio Grande had KGE values of .57, .65 and .77, respectively (lower row of subplots in Figure 2). In order to observe how well the WRF model is simulating weather events that make up the longer-term climate, WRF was forced with the NCEP-NCAR Final Analyses data set which has a resolution of 1x1 degree grids. Using the resulting dynamically downscaled NCEP-NCAR-WRF data to force VIC (at 1/8x1/8 degree grids) for the years 1979-2000, we obtain KGEs of .55, .64, and .74 for the Salt, Verde and Rio Grande, respectively. Therefore, WRF is clearly doing well in reproducing weather events and their timing.

Figure 3 shows examples of the effectiveness of the bias correction. Figure 3a shows the cumulative gamma distribution of the raw, dynamically-downscaled HadCM3 OLTP data (for January 31st) in green while the observed distribution is the black dashed

line. After bias correcting the precipitation, we have the distribution shown by the blue line. The bias corrected distribution is seen to be very similar to the observed distribution. Figure 3b illustrates, for temperature, how we have treated the OLTP and the PJTP differently. Again the green line is the raw HadCM3 data (for January 13th). The figure shows how means are shifted up and the trends are preserved in each period. In this particular case, the variance was only slightly increased in the OLTP to match observations.

The resulting distributional changes before and after bias correction are shown in Figure 4. The upper three rows show the α parameter for the precipitation distributions and the mean for the distributions corresponding to maximum temperature, minimum temperature and wind. The lower three rows show the β parameter for the precipitation distributions and the standard deviation for the distributions corresponding to the other climate variables. The x-axis is the sorted elevation values in the Salt river basin. The y-axis is the days of the year with the beginnings of each month being labeled. The first and fourth rows show the α or mean values and the β or standard deviation values, respectively, prior to bias correction of the HadCM3 model. The second and fifth rows show the same distributional values but for the observed data. The third and sixth rows show the distributional values after bias correcting the HadCM3 climate data. In essence, we want the climatological distributions of each gridcell in the Salt river basin (x-axis), throughout the year (y-axis) to as closely match observations as possible. This means that it is desirable to have the second and third rows for each column to be relatively

indistinguishable from one another. Similarly, rows five and six should look very similar. As an example, it can be seen that prior to bias correction the mean minimum temperature (subplot is row one, column three) was too high especially at higher elevations in the warmer months (top of subplot for months of June, July, August and September). In August at high elevations, the HadCM3 model had a mean minimum temperature near 15°C, while the observations had a mean minimum temperature near 6°C. During the same time of year and at the same elevations in the Salt, the standard deviation of the minimum temperature is being underestimated. In August at high elevations, the HadCM3 model had a standard deviation for the minimum temperature near 1°C, while the observations had a standard deviation near 2°C. It can clearly be seen how closely rows two and three, as well as five and six, resemble each other. Visually, after bias correction the climatological distributions of the HadCM3 model are very close to the observed distributions. How much improvement in quantitatively representing the climatology can be seen by bias correcting the climate data?

Mean absolute error was used to quantify the improvement in matching the observed distributions in the OLTP due to bias correction. The mean absolute error (MAE) is the average of the absolute difference between each value in the sorted empirical distributions (using the 21-day moving windows). Smaller MAE values indicate that the observed and simulated distributions are closer to one another than with larger MAE values. MAE is an open ended scale above zero, so we would like to see a substantial improvement in the reduction of MAE values due to bias correction. Figure 5

shows the change in MAE before and after the bias correction. The left column shows the MAE values between the raw HadCM3 and observed data. Similarly to Figure 4, the x-axis is the sorted elevation values in the Salt river basin, while the y-axis is the days of the year with the beginnings of each month being labeled. The colorbar is logarithmic values of MAE. Figure 5 illustrates substantial reductions in the MAE as a result of bias correcting the HadCM3 model for the Salt river basin. Table 1 provides the spatial (y-axis of Figure 5) and temporal (x-axis of Figure 5) averages of the MAE values for each climate variable using both models for the three basins. For example, the average MAE for the top left subplot (raw precipitation) in Figure 5 is 1.95mm. After bias correction, the MAE is reduced to .38mm. Overall, the precipitation MAE is reduced, on average, across the three basins for the two models by 84%. The maximum temperature, minimum temperature, and wind MAE values were reduced by 92%, 94% and 96%, respectively.

b) Projected Climate Change

Now that the bias corrected HadCM3 and MPI models are more accurately simulating the seasonal climate patterns and distributions, how is the climate in these basins expected to change in the future due to the A1B (“Business as Usual”) climate change scenario? The upper row of Figure 6 shows the the percentage change in average precipitation in the PJTP with respect to the OLTP. The x and y-axes are again the same as in Figures 4 and 5. The bottom two rows of Figure 6 are the differences in average maximum and minimum temperature, respectively. The HadCM3 model is projecting

more precipitation in the January and June months for the time period 2011-2079 with respect to the period 1968-2010. While late April and November months are projected to be drier. The MPI model is, on average projecting a future with less precipitation (for the time period 2011-2080 with respect to the period 1950-2010). Both models are projecting, on average, between a 1°C and 3°C increase in temperature. Changes in wind in the future time period were negligible with respect to the past period. How do these changes in precipitation and temperature translate to differences in anticipated future water availability?

c) Projected Hydrologic Change

Figure 7 illustrates how the probability of exceedance plots change for streamflow between the PJTP and the OLTP. The blue lines show how each projected future streamflow value (expressed as a probability of exceedance on the x-axis) changes with respect to historical flows (y-axis is percentage change). The black, dotted lines are the average percentage changes in overall streamflow. For example, forcing the VIC model with HadCM3 in the Salt, approximately a 35% decrease in streamflow at 10% exceedance values (high flows) is projected for future flows with respect to what has historically been observed. Projected future climate, with both the HadCM3 and MPI models, show decreased streamflow at all values for all three basins except a slight increase at low flows in the Verde (where VIC is forced by HadCM3). The HadCM3 model is projecting on average a 23%, 20% and 22% decrease in future streamflow for

the Salt, Rio Grande and Verde, respectively. The MPI model is projecting on average a 43%, 31% and 38% decrease in future streamflow for the Salt, Rio Grande and Verde, respectively. Performing a t-test for all six instances (both models for the three basins), the PJTP streamflow means were found to be statistically significantly different ($p < .01$) than the OLTP means. These decreases were found to be in the same range as projected using statistical downscaling for the Salt and Verde basins. Rajagopal et al. (~2013, in review) used BCSD and found approximately a 25% decrease in streamflow in the Salt-Verde river system by the end of the 21st century.

As a comparison and to provide greater context, projected average precipitation changes, for each probability of exceedance, is shown in Figure 8. The amount by which the MPI model is projected to be drier in the future is clearly visible. This clearly translates to the streamflow decreases we see in the three basins for the two models. However, temperature and seasonality play an equally integral role in the streamflow probability of exceedance plots.

Changes in snow water equivalent (SWE) and baseflow appear to explain these projected changes to streamflow in the three basins. Figure 9 shows critical components to the water budget as simulated by VIC for the Salt. Spatially and temporally averaging evaporation and surface runoff for HadCM3, there is no clear direction of change for the PJTP with respect to the OLTP. While for MPI, there is less surface runoff but also less evaporation. It can clearly be seen that the substantial percentage decreases in SWE and baseflow are dominating the decreases that are being projected in overall streamflow.

4. Discussion and Conclusions

This study set out to observe if climate projections in the Southwest, under the A1B scenario, would have any discernible effects on the hydrology. With the state of the science, we found that there is indeed a noticeable effect. As a first step, we found that both GCMs, after downscaling, consistently projected future temperatures to increase between a 1°C and 3°C throughout the year at all elevations in the Salt, Verde and Rio Grande basins. Additionally, precipitation is not projected to change in any substantial way for the HadCM3 model, while the MPI is projecting a future with slightly less precipitation on average.

When these dynamically downscaled, bias corrected climate variables from both GCMs are used to force the VIC hydrologic model, statistically significant decreases in streamflow were observed for all three basins. On average, the HadCM3 model projects a 22% decrease in streamflow across the three subbasins, while the MPI projects a 37% decrease. Thus, even with the HadCM3 model, which is projecting approximately the same amount of future precipitation, substantial decreases in streamflow are expected. This is due to significant reductions in SWE and baseflow across the basins in the future.

To extend this research, additional GCM models can be downscaled with more climate change scenarios. This can shed light on the full distribution of projected future streamflow amounts, and provide insight as to whether these initial projections are near the median or the extremes of expected water resources under a changing climate. Also,

the RCMs could be run at a higher resolution (<32km), thereby better resolving certain physical processes (e.g., convective precipitation). Lastly, further investigation is required to understand why the low flows of the Rio Grande headwaters are projected to change so differently than those of the Salt and the Verde. This could be due to the difference between the VIC model calibration for the Rio Grande and the Salt/Verde. Figure 2 shows that the calibrated VIC model for the Rio Grande simulates a much steeper streamflow response to changes in precipitation and/or temperature than that of the observed streamflow. Therefore, small changes in Rio Grande precipitation and/or temperature can lead to more substantial changes in projected streamflow than for the Salt or Verde.

Past studies have shown that climate change will alter the timing of streamflow due to warmer temperatures and earlier snowmelt (Barnett et al., 2005; Cayan, 2000; Stewart et al., 2004). Given the importance of an already stressed resource in the Southwest, it is imperative to understand how the total volume of water may also change. With an initial set of models, using the A1B climate change scenario, the streamflows of the Southwest appear to be under threat. More studies that expand upon these results using additional model runs will fill in the distribution of possible futures. However, before access to all of those results are obtained, water managers should think about setting contingency plans for a drier Southwest.

References

- Acharya, A., T. C. Piechota, and G. Tootle, 2012: Quantitative Assessment of climate change impacts on the hydrology of the North Platte river watershed, Wyoming. *J. Hydrol. Eng.*, **17**, 1071-1083.
- Allen, M. R., and W. J. Ingram, 2002: Constraints on future changes in climate and the hydrologic cycle. *Nature*, **419**, 224-232.
- Bárdossy A., and G. Pegram, 2011: Downscaling precipitation using regional climate models and circulation patterns toward hydrology. *Water Resour. Res.*, **47**, W04505, doi:10.1029/2010WR009689.
- Barnett, T. P., J. C. Adam, and D. P. Lettenmaier, 2005: Potential impacts of a warming climate on water availability in snow-dominated regions. *Nature*, **438**, 303-309.
- Castro, C. L., R. A. Pielke Sr., and G. Leoncini, 2005: Dynamic downscaling: assessment of value retained and added using the regional atmospheric modeling system (RAMS). *J. Geophys. Res.*, **110**, D05108, doi:10.1029/2004JD004721.
- Cayan, D. R., S. A. Kammerdiener, M. D. Dettinger, J. M. Caprio, and D. H. Peterson, 2001: Changes in the onset of spring in the western United States. *BAMS*, **82** (3), 399-415.
- Christensen, N. S., A. W. Wood, N. Voisin, D. P. Lettenmaier, and R. N. Palmer, 2004:

- The effects of climate change on the hydrology and water resources of the Colorado river basin. *Climate Change*, **62**, 337-363.
- Dominguez, F., E. Rivera, D. P. Lettenmaier, and C. L. Castro, 2012: United States under a warmer climate as simulated by regional climate models. *Geophys. Res. Lett.*, **39**, L05803, doi:10.1029/2011GL050762.
- Frich, P., L. V. Alexander, P. Della-Marta, B. Gleason, M. Haylock, A. M. G. Klein Tank, and T. Peterson, 2002: Observed coherent changes in climatic extremes during the second half of the twentieth century. *Clim. Res.*, **19**, 193-212.
- Gao, Y., J. A. Vano, C. Zhu, and D. P. Lettenmaier, 2011: Evaluating climate change over the Colorado river basin using regional climate models. *J. Geophys. Res.*, **116**, D13104, doi:10.1029/2010JD015278.
- Gupta, H. V., H. Kling, K. K. Yilmaz, and G. F. Martinez, 2009: Decomposition of the mean squared error and NSE performance criteria: implications for improving hydrological modeling. *J. Hydrol.*, **377**, 80-91.
- Hamlet, A. F., and D. P. Lettenmaier, 1999: Effects of climate change on hydrology and water resources in the Columbia river basin. *J. Am. Water Resour. As.*, **35 (6)**, 1597-1623.
- Held, I. M., and B. J. Soden, 2006: Robust responses of the hydrological cycle to global warming. *J. Climate*, **19**, 5686-5699.
- Karl, T. R., K. E. Trenberth, 2003: Modern global climate change. *Science*, **302**, 1719-1723.

- Maurer, E. P., A. W. Wood, J. C. Adam, D. P. Lettenmaier, and B. Nijssen, 2002: A long-term hydrologically based dataset of land surface fluxes and states for the conterminous United States. *J. Climate*, **15**, 3237-3251.
- Maurer, E. P., and H. G. Hidalgo, 2008: Utility of daily vs. monthly large-scale climate data: an intercomparison of two statistical downscaling methods. *Hydrol. Earth Syst. Sci.*, **12**, 551-563.
- Milly, P. C. D., K. A. Dunne, and A. V. Vecchia, 2005: Global pattern of trends in streamflow and water availability in a changing climate. *Nature*, **438** (17), 347-350.
- Milly, P. C. D., J. Betancourt, M. Falkenmark, R. M. Hirsch, Z. W. Kundzewicz, D. P. Lettenmaier, and R. J. Stouffer, 2008: Stationarity is dead: whither water management? *Science*, **319**, 573-574.
- Murphy, J., 2000: Predictions of climate change over Europe using statistical and dynamical downscaling techniques. *Int. J. of Climatol.*, **20**, 489-501.
- Stewart, I. T., D. R. Cayan, and M. D. Dettinger, 2004: Changes in snowmelt runoff timing in western north america under a 'business as usual' climate change scenario. *Climate Change*, **62**, 217-232.
- Stewart, I. T., D. R. Cayan, M. D. Dettinger, 2005: Changes toward earlier streamflow timing across western north America. *J. Climate*, **18**, 1136-1155.
- Sungwook, W., F. Dominguez, M. Durcik, J. Valdes, H. F. Diaz, and C. L. Castro, 2012: Climate change projection of snowfall in the Colorado river basin using dynamical downscaling. *Water Resour. Res.*, **48**, W05504, doi:10.1029/2011WR010674.

- Teutschbein, C. and J. Seibert, 2012: Bias correction of regional climate model simulations for hydrological climate-change impact studies: review and evaluation of different methods. *J. Hydrol.*, **456-457**, 12-29.
- Vano, J. A., T. Das, and D. P. Lettenmaier, 2012: Hydrologic sensitivities of colorado river runoff to changes in precipitation and temperature. *J. Hydrometeorol.*, **13**, 932-949.
- Von Storch, H., E. Zorita, and U. Cubasch, 1993: Downscaling of global climate change estimates to regional scales: an application to Iberian rainfall in wintertime. *J. Climate*, **6**, 1161-1171.
- Wilby, R. L., T. M. L. Wigley, D. Conway, P. D. Jones, B. C. Hewitson, J. Main, and D. S. Wilks, 1998: Statistical downscaling of general circulation model output: a comparison of methods. *Water Resour. Res.*, **34 (11)**, 2995-3008.
- Wood, A. W., L.R. Leung, V. Sridhar, and D. P. Lettenmaier, 2004: Hydrologic implications of dynamical and statistical approaches to downscaling climate model outputs. *Climate Change*, **62**, 189-216.

Tables

	Precipitation (mm)		Max Temp (°C)		Min Temp (°C)		Wind (m/s)	
	Raw	BC	Raw	BC	Raw	BC	Raw	BC
Salt-HadCM3	1.95	.38	2.99	.27	4.09	.27	2.40	.12
Salt-MPI	3.60	.36	4.37	.27	4.16	.28	3.03	.11
Verde-HadCM3	1.89	.35	3.46	.28	3.90	.28	2.56	.09
Verde-MPI	3.19	.31	4.85	.27	3.52	.28	3.27	.07
Rio-HadCM3	2.02	.48	2.76	.32	6.28	.27	2.12	.14
Rio-MPI	1.84	.41	4.03	.41	5.54	.28	2.82	.12

Table 1: The Mean Absolute Error (MAE) values of the raw climate variables and after they were bias corrected (BC).

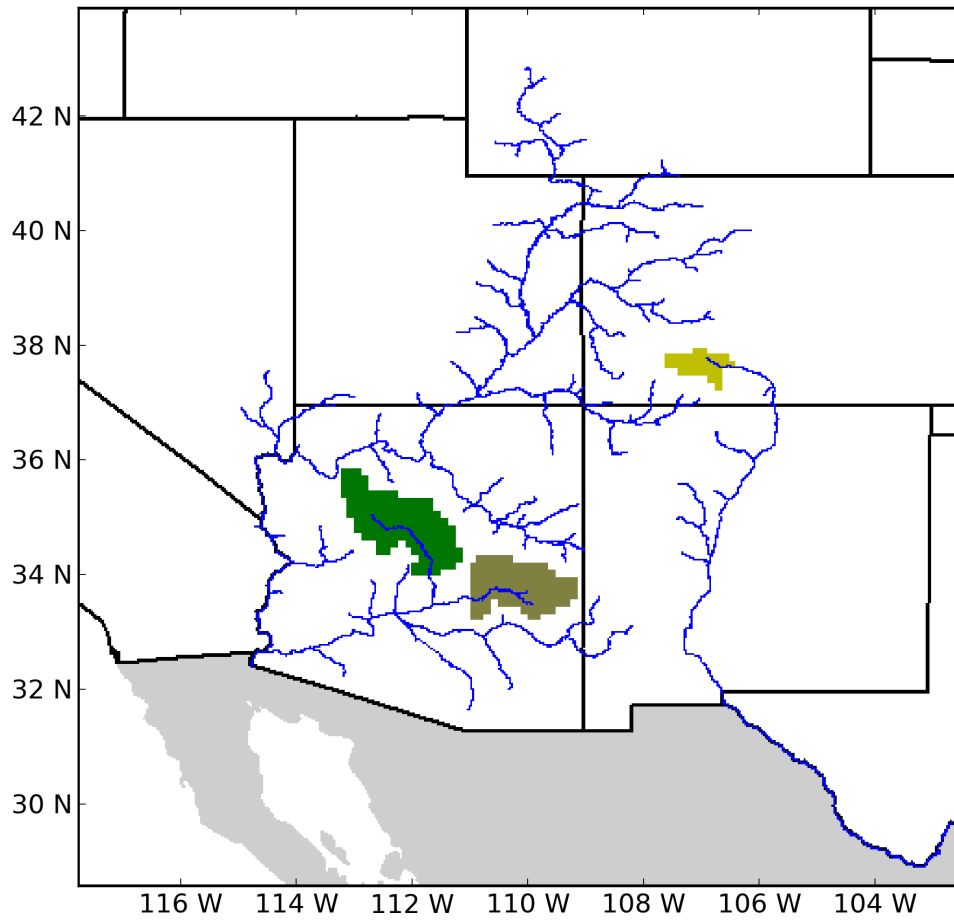
Figures

Figure 1: The three basins used are the Verde (green), Salt (tan), and the Rio Grande headwaters (gold).

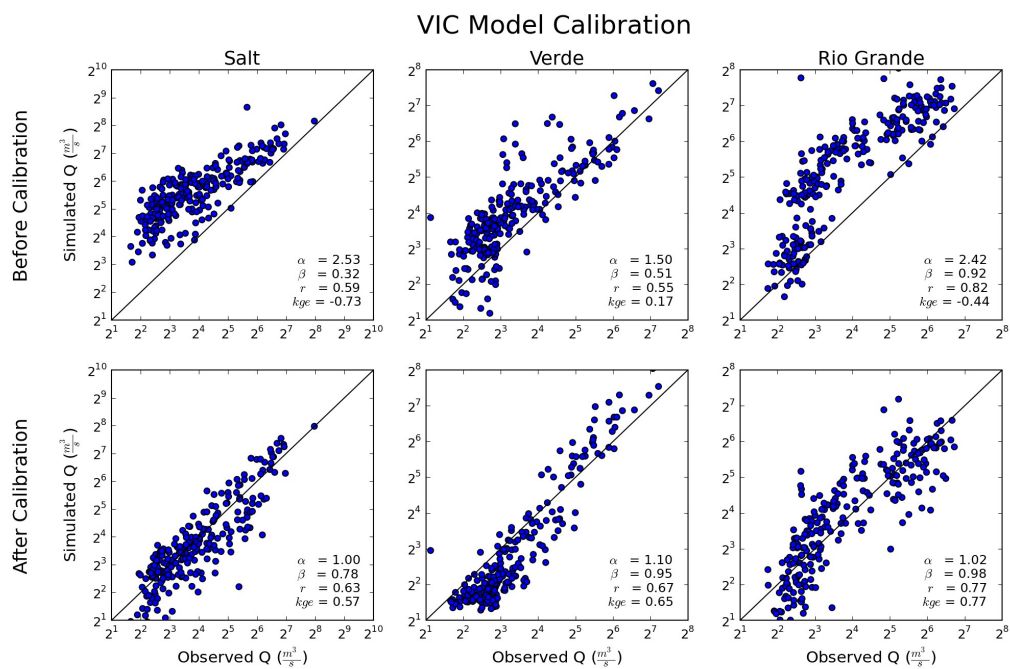


Figure 2: Observed versus simulated streamflows before and after calibration. All components of the KGE as well as the value itself are inset. Substantial reductions in the bias can be seen for the Salt and Rio Grande basins.

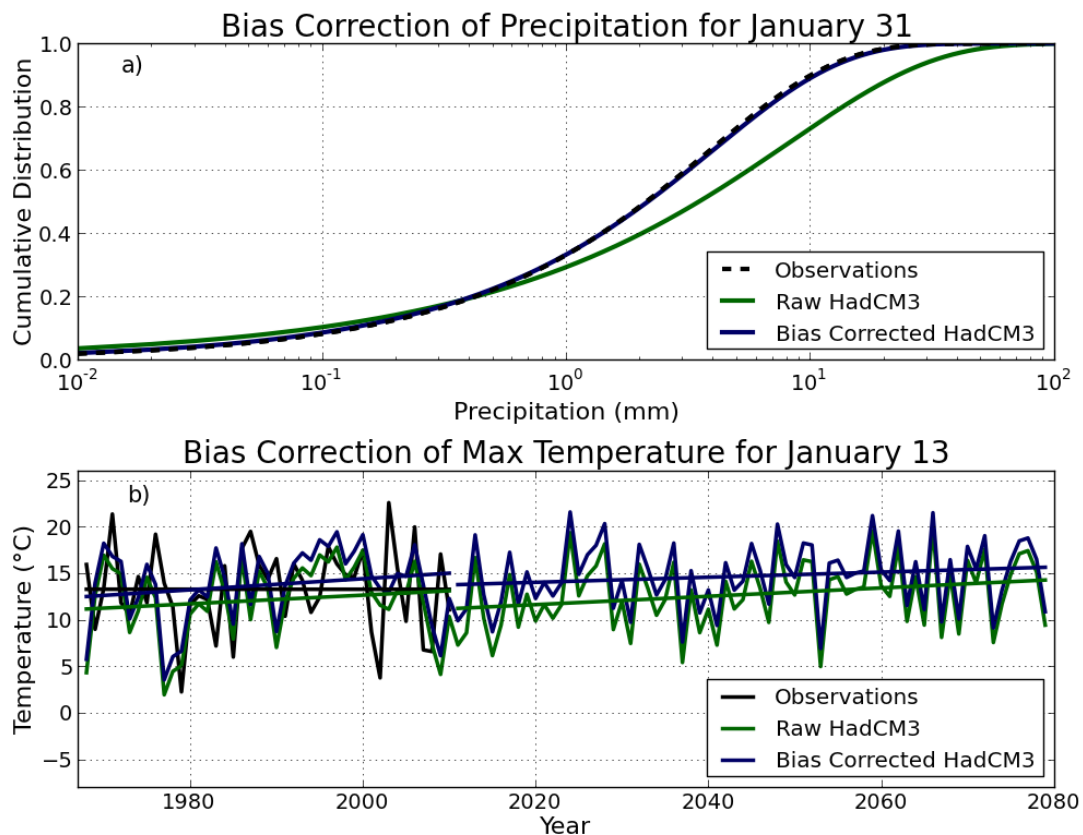


Figure 3: Subplot a) shows the shifting of the HadCM3 precipitation CDF, due to bias correction, for the example date of January 31st. Fitted observations are the dashed black line, the raw fitted data is the green line, and the bias corrected fit is the blue line. Subplot b) shows the time series of bias corrected max temperature for all January 13th days. The means and variances are shifted to match observations, while the trends are preserved.

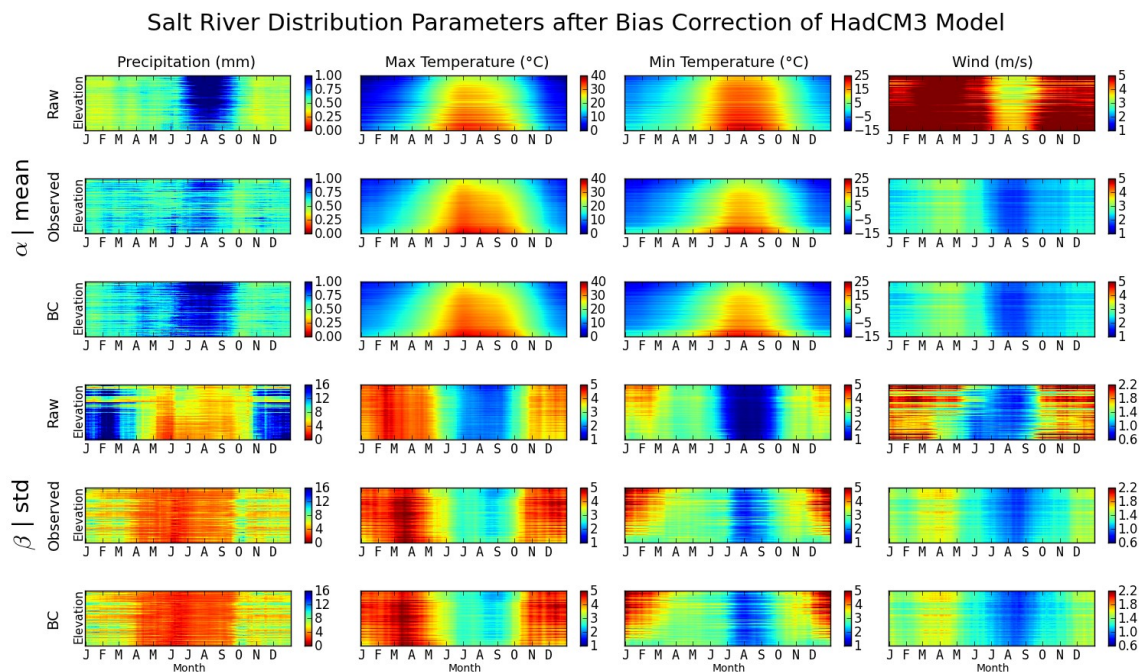


Figure 4: The raw distribution parameters α and mean correspond to the upper three rows of subplots, while β and standard deviation correspond to the bottom three rows. The first and fourth rows show the raw distribution parameters. The second and fifth rows show the observed parameters. The third and sixth rows show the bias corrected parameters. The x-axis are the days of the year with the months shown. The y-axis is sorted elevation for the Salt river, with the highest elevation on top. Ideally, if the bias corrected variable had very similar distributions to observations, rows two and three should like identical and similarly for five and six.

Mean Absolute Error in the Salt River after Bias Correction of HadCM3 Model

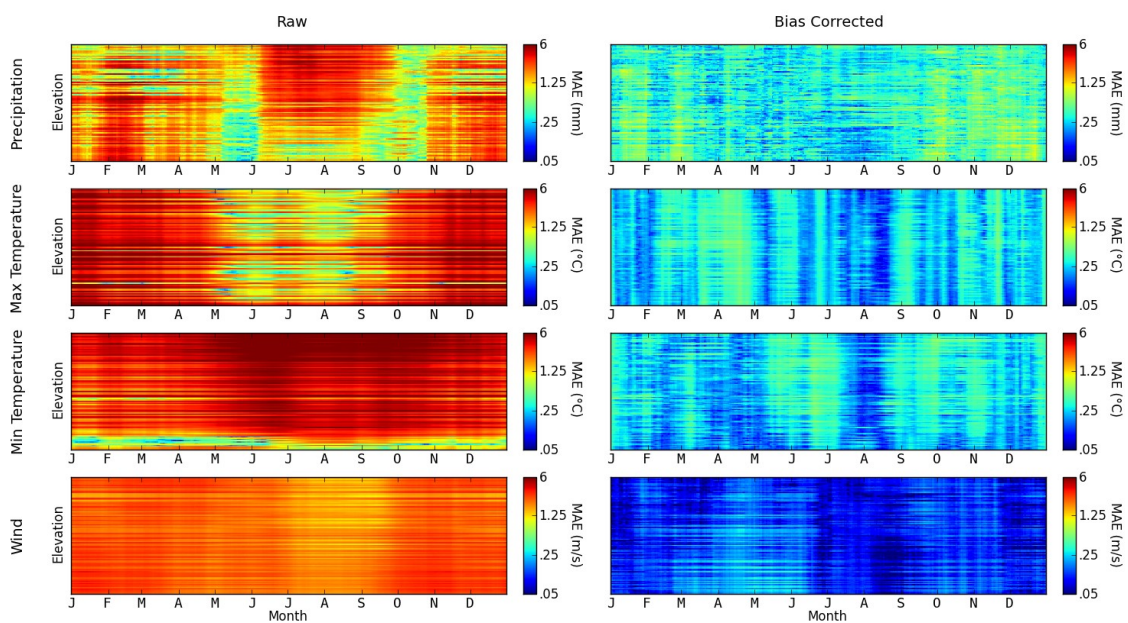


Figure 5: Example of the Mean Absolute Errors for the raw climate variables and after bias correction. The x and y-axes are the same as figure 4. The colorbars are logarithmic.

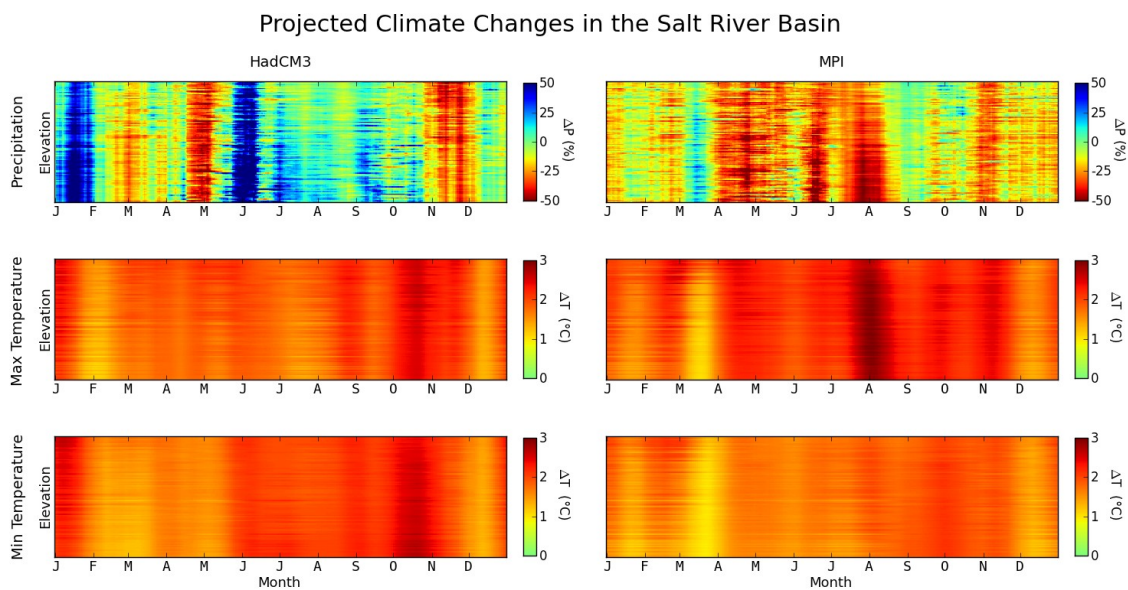


Figure 6: Projected climate changes in the Salt river basin for both the HadCM3 and MPI models. The x and y axes are same as Figures 4 and 5. The colorbars for precipitation show the percentage change in projected future values with respect to past values. The temperature colorbars show the difference between projected future values with respect to past values.

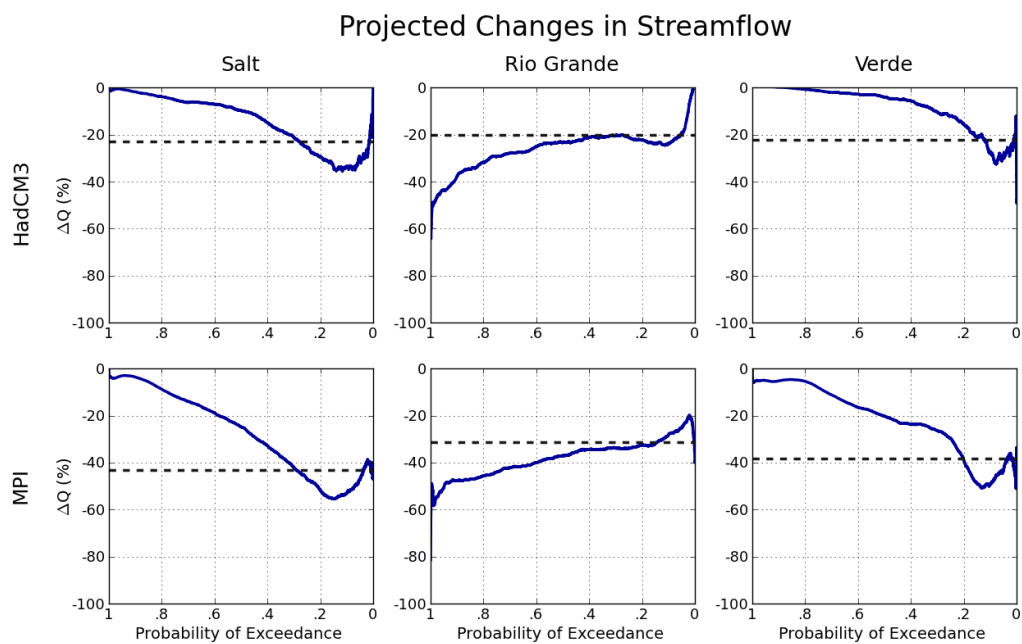


Figure 7: Projected average streamflow changes, for each probability of exceedance, in reference to the modeled data prior to the year 2011. Both models are projecting greater decreases at low flows than at high flows for the Salt and Rio Grande, while the opposite is true for the Verde.

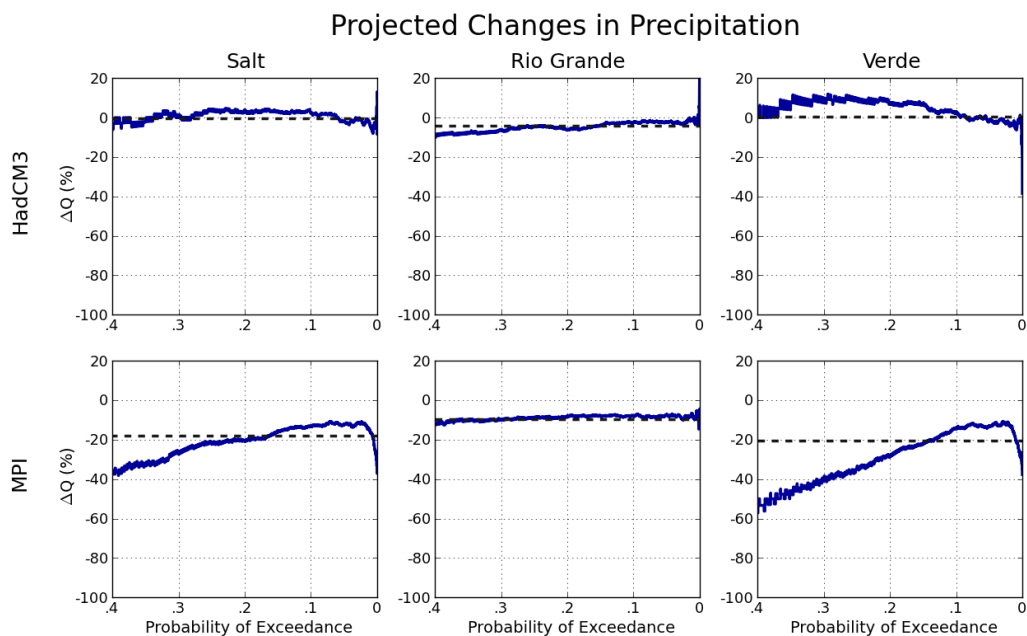


Figure 8: Projected average precipitation changes, for each probability of exceedance, in reference to the modeled data prior to the year 2011. Higher exceedance values are not shown because many days have no precipitation at all. A 40% exceedance value corresponds to negligible to low precipitation values, in the OLTP, across the basins (~ 0.3 mm for the Salt, ~ 1 mm for the Rio Grande headwaters, and ~ 0.2 mm for the Verde). The amount by which the MPI model is projected to be drier in the future is clearly visible.

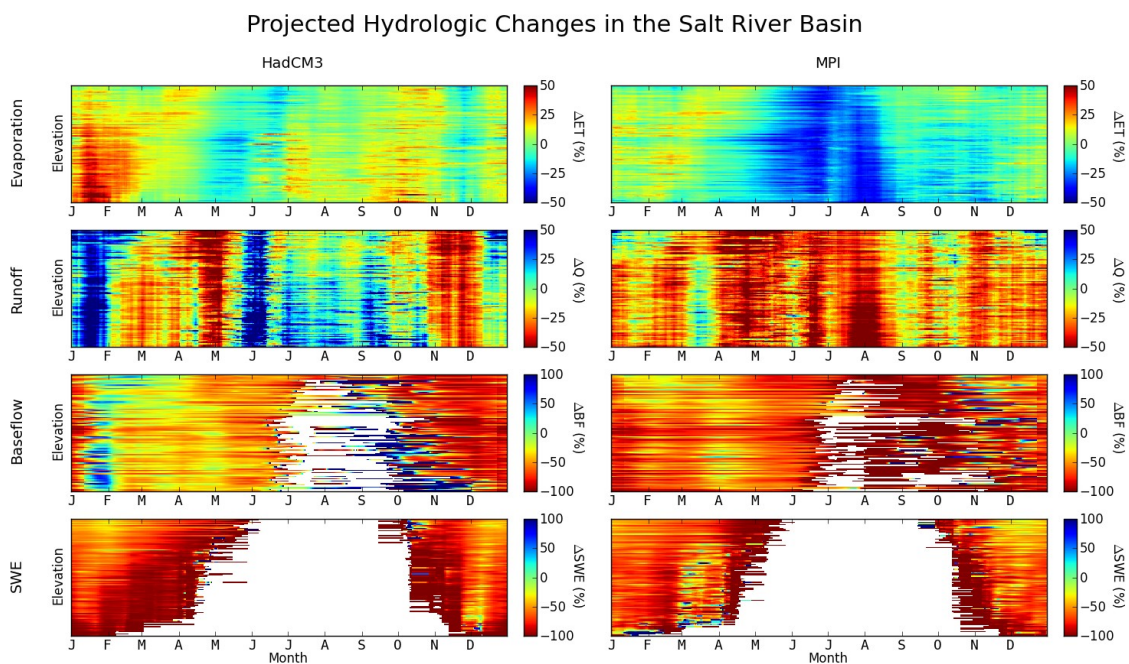


Figure 9: Projected hydrologic changes in the Salt river basin for both the HadCM3 and MPI models. These variables were obtained from the VIC model. The colorbars show the percentage changes of the projected future values with respect to the past values. The variables are evaporation, runoff, baseflow and snow water equivalent (SWE), respectively.